

Gefitinib-Tamoxifen Hybrid Ligands as Potent Agents against Triple-Negative Breast Cancer

Carine M. Abdelmalek, Zexi Hu, Thales Kronenberger, Jenni Küblbeck, Franziska J. M. Kinnen, Salma S. Hesse, Afsin Malik, Mark Kudolo, Raimund Niess, Matthias Gehringer, Lars Zender, Paula A. Witt-Enderby, Darius P. Zlotos,* and Stefan A. Laufer*



Cite This: *J. Med. Chem.* 2022, 65, 4616–4632



Read Online

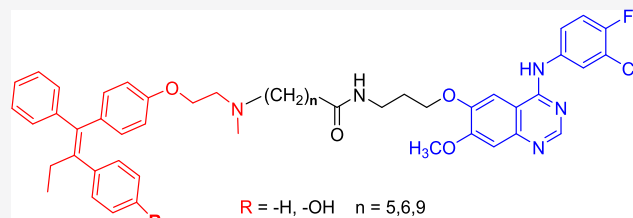
ACCESS |

Metrics & More

Article Recommendations

Supporting Information

ABSTRACT: Anticancer drug conjugates may benefit from simultaneous action at two targets potentially overcoming the drawbacks of current cancer treatment, such as insufficient efficacy, high toxicity, and development of resistance. Compared to a combination of two single-target drugs, they may offer an advantage of pharmacokinetic simplicity and fewer drug–drug interactions. Here, we report a series of compounds connecting tamoxifen or endoxifen with the EGFR-inhibitor gefitinib via a covalent linkage. These hybrid ligands retain both ER antagonist activity and EGFR inhibition. The most potent analogues exhibited single-digit nanomolar activities at both targets. The amide-linked endoxifen-gefitinib drug conjugates **17b** and **17c** demonstrated the most favorable anti-cancer profile in cellular viability assays on MCF7, MDA-MB-231, MDA-MB-468, and BT-549 breast cancer cells. Most importantly, in TNBC cells **17b** and **17c** displayed nanomolar IC₅₀-values (380 nM – 970 nM) and were superior in their anti-cancer activity compared to their control compounds and combinations thereof.



17b

(R = OH, n = 5)

ER_α IC₅₀ = 4.6 nM

EGFR IC₅₀ = 2.5 nM

TNBC cells IC₅₀ = 460–889 nM

INTRODUCTION

Hybrid anticancer agents (anticancer drug conjugates) are an emerging approach to overcome drawbacks of current anticancer treatment, such as insufficient potency and efficacy, high toxicity, and development of resistance.^{1,2} In drug conjugates, two drugs (pharmacophores) are combined in one molecule exerting simultaneous action on at least two different targets.³ In comparison to a combination of two single-target drugs, drug conjugates may offer an advantage of less complex pharmacokinetics and fewer drug–drug interactions.⁴ Drug conjugates should be distinguished from antibody-drug conjugates (ADCs), which are monoclonal antibodies linked to pharmacologically active (typically cytotoxic) small molecules. While ADCs have been successfully introduced as cancer therapeutics,⁵ hybrid drug anticancer agents have mostly been reported in preclinical studies.⁴ However, the number of publications in this field has constantly increased in the last two decades. Indeed, a PubMed data search using the term “anticancer hybrids” revealed the number of relevant publications to have risen from 33 in 1996 to 393 in 2020.⁶ To the best of our knowledge, the only anticancer drug conjugate that reached phase I clinical trials is CUDC-101, a dually acting chimeric EGFR/HDAC inhibitor derived from erlotinib and vorinostat,^{7,8}

Most series of anticancer drug conjugates target breast cancer, as recently reviewed.⁹ Breast cancer is the most common malignancy among women. Approximately 70% of breast cancers are estrogen-receptor positive (ER+).¹⁰ The ER-antagonist tamoxifen belongs to the most common endocrine therapies against ER+ breast cancer. However, its chronic use can increase the risk of uterine cancer¹¹ and induce tamoxifen resistance.¹² Hybrid ligands combining tamoxifen and related compounds with other classes of anticancer agents may be beneficial for future treatment of breast cancer and help offset the adverse effects of tamoxifen usage alone.⁹ Indeed, drug conjugates combining tamoxifen with other drugs, such as doxorubicin,¹³ melatonin,¹⁴ and the HDAC-inhibitor vorinostat,^{15,16} have been reported (Figure 1).

Protein kinases are emerging targets in breast cancer treatment.¹⁷ Resistance to endocrine therapy in ER+ breast cancer has been associated with overexpression and increased activity of receptor tyrosine kinases including insulin-like growth

Received: September 20, 2021

Published: March 14, 2022



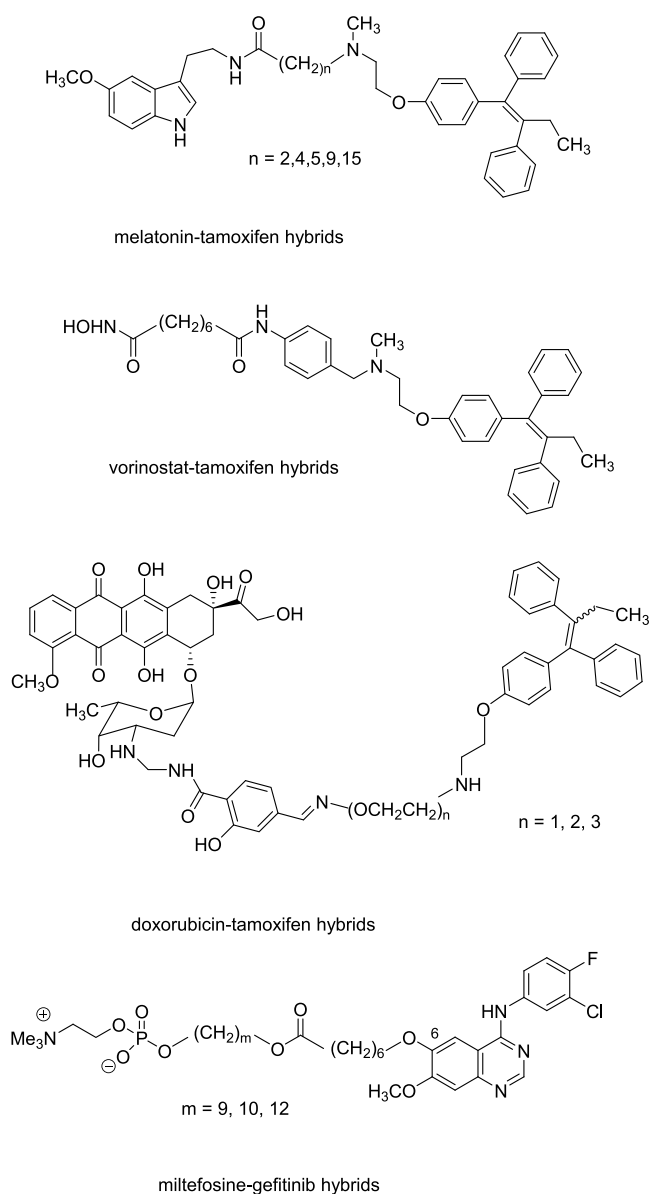


Figure 1. Structures of previously reported anticancer drug conjugates incorporating either tamoxifen or gefitinib.

factor receptor (IGFR),¹⁸ epidermal growth factor receptor (EGFR/HER1), and human epidermal growth factor receptor 2 (HER2).^{19,20} Indeed, gefitinib, an EGFR inhibitor with moderate off-target activity on HER2, was reported to reverse tamoxifen resistance in tamoxifen-resistant MCF-7 cells by up-regulating ER mRNA levels and inducing re-expression of ER α .²¹ Moreover, the combination of gefitinib and 4-hydroxytamoxifen, a tamoxifen metabolite with increased activity, synergistically increased apoptosis in EGFR-positive and ER+ breast cancer *in vitro* (BT474 breast cancer cells) and *in vivo* (xenograft mouse) models.²² Analysis of clinical data from >2000 patients with ER+ breast cancer treated with tamoxifen revealed that aberrant EGFR expression was associated with poor prognosis suggesting that EGFR inhibition may be an adjuvant therapeutic strategy for treating hormone receptor-positive breast cancer.²²

For previously reported drug conjugates, EGFR-inhibitors have been frequently combined with histone deacetylase

inhibitors.²³ Recently, alkylphosphocholine-gefitinib anticancer hybrids have been reported.²⁴

Here, we describe a series of drug conjugates combining tamoxifen and its active metabolite endoxifen with gefitinib via a covalent linkage. The results reveal that these hybrid ligands retain both ER α binding affinity and EGFR inhibition. Moreover, some of the drug conjugates proved to be superior to the parent drugs in their potency/efficacy to inhibit viability and migration in four diverse breast cancer cell lines.

RESULTS AND DISCUSSION

Design and Synthesis of Tamoxifen-Gefitinib Drug Conjugates. Hybrid ligand design started from the X-ray crystal structure of 4-hydroxytamoxifen bound to the ligand binding domain of ER α (PDB 3ERT). The structure revealed the dimethylamino group to be solvent exposed making the latter a suitable attachment point for the linker (Figure 2).

Of note, this group has also been used as an attachment point for the linker in previously reported tamoxifen-vorinostat drug conjugates (Figure 1).¹⁵ Consequently, the same type of *N*-alkyl linkage has been chosen for the gefitinib-tamoxifen hybrid ligands described here. On the gefitinib side, the 6-alkoxy moiety was chosen as the linkage point since the crystal structures of gefitinib-EGFR complexes (PDB codes 3UG2 and 4WKQ) showed the *O*-morpholinopropyl group at C6 to extend outside the ATP binding pocket toward the solvent. Indeed, 6-alkoxy-linked hybrid ligands of gefitinib and miltefosine (Figure 1) were reported to retain EGFR inhibition (70–87% at 1 μ M).²⁴ For the initial series of tamoxifen-gefitinib hybrids 5a–e (Scheme 1), alkyl amide linkers ($CH_2)_n - NHCO$ ($n = 4–6, 9, 15$) similar to those in the previously reported tamoxifen-melatonin drug conjugates (Figure 1) have been used. Additionally, ethylene glycol linkers ($CH_2 - CH_2 - O -$), $n = 1, 2$, have been incorporated in drug conjugates 7a and 7b (Scheme 2).

The synthetic approaches toward 5a–e and 7a,b are shown in Schemes 1 and 2, respectively. The hybrid ligands 5a–e with an amide function incorporated into the spacer were prepared from nortamoxifen in a three step approach involving *N*-alkylation with $Br(CH_2)_nCO_2R$ ($R = Me$ or Et) to give intermediates 1a–e followed by ester hydrolysis to give the corresponding acids 2a–e, and final amide coupling with the primary amine 4. The latter was obtained from desmorpholinopropyl gefitinib by *O*-alkylation with $BocNH(CH_2)_3Br$ to give ether 3 followed by acid-promoted Boc deprotection (Scheme 1). The hybrid ligands 7a and 7b with one and two ($CH_2 - CH_2 - O -$) units in the spacer were prepared in two steps from desmorpholinopropyl gefitinib. *O*-alkylation of the latter with di-iodoalkylethers I- $(CH_2CH_2O)_nCH_2CH_2-I$ ($n = 1$ or 2 , respectively) gave 6a and 6b, which, in turn, were used for *N*-alkylation of nortamoxifen to give 7a and 7b (Scheme 2).

Pharmacological Characterization of Tamoxifen-Gefitinib Drug Conjugates. The affinity of our hybrid ligands 5a–e and 7a,b for the human ER α was first evaluated in a commercial radioligand binding assay (Eurofins Cerep, France), as previously reported.²⁵ Briefly, ER α expressed in transfected Sf9 cells was incubated with 0.5 nM [3H]-estradiol in the absence and presence of hybrid ligands at different concentrations (1 μ M, 100 nM, 10 nM, 1 nM). Nonspecific binding was determined in the presence of 1 μ M diethylstilbestrol. The results, expressed as a percent inhibition of the radioligand-specific binding, are shown in Table 1.

Like tamoxifen, all tamoxifen-gefitinib drug conjugates show concentration-dependent inhibition of [3H]estradiol-binding to

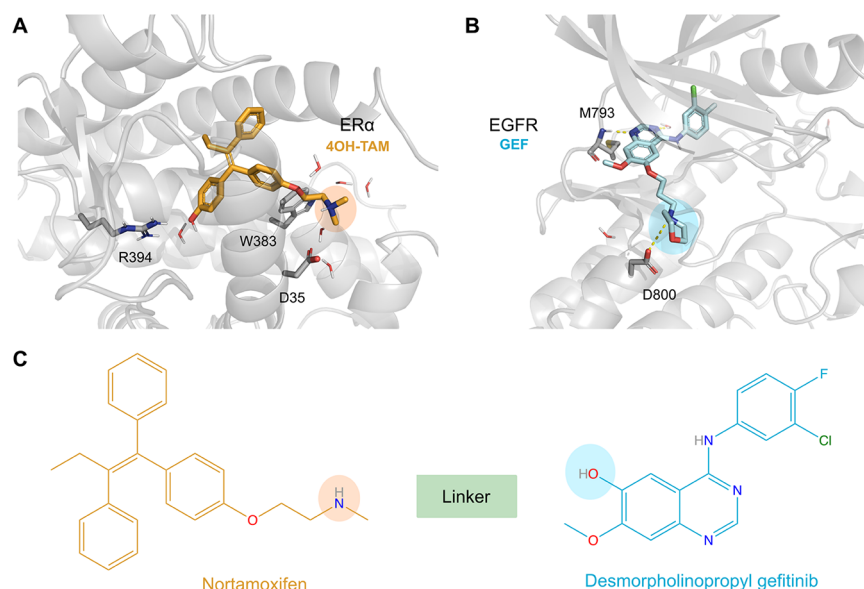


Figure 2. Modification sites of both parent drugs are solvent exposed in both targets. (A) ER α crystal structure with 4-OH-tamoxifen bound (PDB ID: 3ERT); the amino group extends beyond the disordered helix 12. (B) EGFR crystal structure with gefitinib bound (PDB ID: 4WKQ); the morpholine ring extends to the solvent-exposed front region and is located far from the key interaction points, such as the hinge region. (C) 2D schematic representation of the initial compounds and their respective sites of modification.

ER α with the highest [3 H]estradiol-displacement reaching nearly 100% at 1 μ M for most of the analogues. The binding affinity in the series of $(\text{CH}_2)_n\text{-NHCO}$ -linked hybrid ligands **5a–e** ($n = 4–6, 9, 15$, respectively) is dependent on the length of the linker. As best seen at 10 nM concentration, hybrid ligands with the shortest and longest spacers **5a** ($n = 4$) and **5e** ($n = 15$), respectively, show only moderate affinity (38.8 and 34.3% inhibition of estradiol binding) relative to tamoxifen (64.4%). In contrast, **5d** ($n = 9$) and, to a lesser extent, **5c** ($n = 6$) are characterized by higher affinity (78.5 and 68.7% inhibition of estradiol binding) than tamoxifen. The ethylene glycol-linked drug conjugates **7a** and **7b** also show lower affinity than tamoxifen (26.9 and 33.6% inhibition of estradiol binding).

The ER α antagonist activity of **5a–e** and **7a,b** was subsequently determined as their ability to antagonize the effect of estradiol in a luciferase reporter assay, as previously reported.^{26,27} Briefly, C3A cells were double transfected with plasmids expressing the human ER α and ERE2-TATA-luciferase (estrogen response elements) and then treated with 10 nM 17 β -estradiol and the hybrid compounds. The estradiol-activated ER α binds to the ERE2 element leading to the luciferase expression, the activity of which is then quantified. The results are shown in Table 2. The concentration-response curves are shown in the Supporting Information (Figure S1).

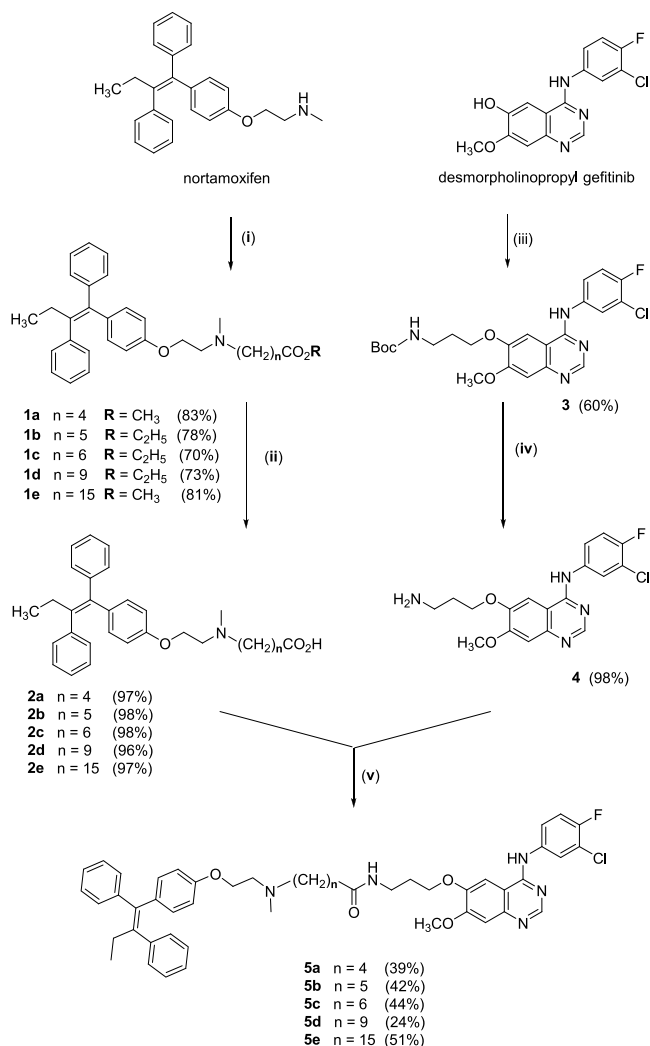
The ER α luciferase reporter assay confirms that all tamoxifen-derived hybrid ligands retain the antagonist effect of the parent drug with variable potencies. As expected, the hybrid ligand **5e** with the longest $(\text{CH}_2)_{15}\text{NHCO}$ -linker separating both pharmacophores that showed the lowest ER α binding affinity in radioligand displacement studies, is found to be the least potent antagonist ($\text{IC}_{50} = 6487$ nM). Drug conjugates with shorter linkers (**5a**, **5b**, **7a**, and **7b**) demonstrate similar antagonist activity ($\text{IC}_{50} = 100$ to 335 nM) being only moderately less potent than tamoxifen ($\text{IC}_{50} = 48.9$ nM). The most potent analogue is the $(\text{CH}_2)_6\text{NHCO}$ -linked hybrid ligand **5c** showing a 5-fold higher antagonist effect than tamoxifen.

Design and Synthesis of Endoxifen-Gefitinib Drug Conjugates. Tamoxifen is a prodrug metabolized by

cytochrome P-450 enzymes into the primary metabolites, *N*-desmethyl-tamoxifen and 4-hydroxytamoxifen. The latter undergoes a further *N*-demethylation to endoxifen that is considered the most important active metabolite.²⁸ 4-Hydroxytamoxifen and endoxifen have comparable antiestrogenic effects and show 30–100-fold higher activity than the parent drug.²⁹

The hybrid ligands **5a–e** and **7a,b** are composed of gefitinib linked to tamoxifen. Based on the higher anti-estrogenic activity of 4-hydroxytamoxifen and endoxifen relative to tamoxifen, the introduction of a hydroxy group into the tamoxifen moiety of the drug conjugates is expected to increase their antagonist potency at ER α . To test this hypothesis, four hybrid ligands with various linkers were structurally modified by replacing their tamoxifen units with 4-hydroxytamoxifen. The modified analogues are derived from three drug conjugates that displayed the highest ER α antagonist potency, namely, **5b** ($\text{IC}_{50} = 100$ nM), **5c** ($\text{IC}_{50} = 11$ nM), and **7b** ($\text{IC}_{50} = 192$ nM), and from the hybrid ligand **5d** that demonstrated the highest affinity toward ER α in the radioligand binding assay.

The structures and synthetic approaches toward the respective hydroxylated ligands **17b**, **17c**, **14**, and **17d** are shown in Schemes 3 and 4. Of note, while **17b–d** are $(\text{CH}_2)_n$ -amide linked analogues ($n = 5, 6$, and 9), the hybrid ligand **14** only includes two $-\text{CH}_2\text{-CH}_2\text{-O}-$ units in the spacer. The starting material for the synthesis of **14** was (*Z*)-endoxifen (**11**). The latter was prepared from 4,4'-dihydroxybenzophenone according to an optimized procedure derived from Milroy *et al.*³⁰ (Scheme 3). Briefly, the key intermediate **8** was subjected to a Mitsunobu reaction with alcohol **9** to give the phenyl alkyl ether **10**. Simultaneous cleavage of the pivalate ester and trifluoroacetamide using LiOH gave (*Z*)-endoxifen (**11**). Subsequent TBDSMS-protection of the phenolic OH-group of **11** resulted in the corresponding TBDSMS-ether **12** that was subjected to *N*-alkylation with intermediate **6b** to give protected drug conjugate **13**. Finally, the silyl group of compound **13** was removed with tetrabutylammonium fluoride in THF followed by neutral aqueous workup to yield the pure (*Z*)-isomer of the

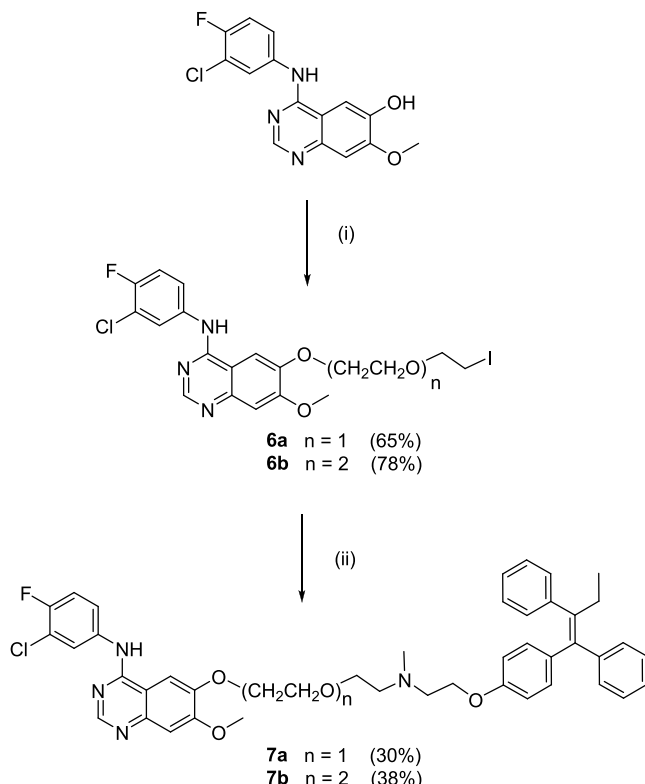
Scheme 1. Structures and Synthesis of 5a–e^a

^aReagents and conditions: (i) NaH, DMF, Br(CH₂)_nCO₂R, rt, 24 h; (ii) 1. LiOH, THF, H₂O, rt, 2. HCl (aq), rt, 24 h; (iii) NaH, DMF, Br(CH₂)₃NHBoc; (iv) 1. TFA, DCM, 2. NaHCO₃ (aq); (v) TBTU, DIPEA, DMF.

hybrid compound 14, as confirmed by HPLC and NMR. Noteworthy, and in contrast to deprotection of intermediate 10, TBDMS cleavage of compound 13 using LiOH·H₂O resulted in partial double bond isomerization (up to 23%) even when neutral conditions were ensured during the workup and purification by column chromatography.

Synthesis of the amide-linked drug conjugates 17b–d (Scheme 4) started with coupling of amine 4 with the acids Br(CH₂)_nCO₂H (n = 5, 6, 9) to yield the amides 15b–d which were used for N-alkylation of the silyl-protected endoxifen 12 to obtain protected drug conjugates 16b–d. A final TBDMS-deprotection using TBAF in THF gave the final compounds 17b–d.

Pharmacological Characterization of Endoxifen-Gefitinib Drug Conjugates. The affinity of compound 14 for the human ER α was initially evaluated in the [³H]-estradiol competition binding assay described previously and compared to 4-hydroxytamoxifen, endoxifen, and the non-hydroxylated analogue 7b (Table 3). As expected, the active metabolites of tamoxifen, 4-hydroxytamoxifen, and endoxifen cause signifi-

Scheme 2. Structures and Synthesis of 7a,b^a

^aReagents and conditions: (i) NaH (60% dispersion), DMF, I-(CH₂CH₂O)_nCH₂CH₂-I, 0° to rt; (ii) NaH (60% dispersion), DMF, nortamoxifen.

Table 1. Estrogen Receptor α Binding Assay^b

compound	% inhibition of 0.5 nM [³ H]estradiol binding at a given concentration			
	1 μ M	100 nM	10 nM	1 nM
tamoxifen	99.2	94.4	64.4	14.1 ^a
5a	98.8	85.8	38.8	1.5 ^a
5b	99.7	94.5	64.9	18.9 ^a
5c	99.7	96.3	68.7	14.4 ^a
5d	99.4	97.2	78.5	29.0
5e	91.2	79.4	34.3	12.4 ^a
7a	99.1	83.9	26.9	7.4 ^a
7b	99.0	83.4	33.6	7.5 ^a

^aInhibition lower than 25% is mostly attributable to variability of the signal around the control level and is not considered significant.

^bValues represent the mean of two independent experiments.

cantly higher radioligand displacement than the parent drug at all concentrations. The same holds true for the hybrid ligand 14 demonstrating higher affinity toward ER α than the non-hydroxylated analogue 7b at 100 and 10 nM concentrations.

The ER α antagonist activity of the hybrid ligands 14 and 17b–d was also tested for their ability to antagonize estradiol/ER α /ERE2-mediated activation of luciferase activity described previously and compared to 4-hydroxytamoxifen, endoxifen, and the respective non-hydroxylated drug conjugates 7b and 5b–d. The results are shown in Table 4.

As expected, 4-hydroxytamoxifen and endoxifen demonstrate much higher antagonist potency (230–349-fold) than tamoxifen. Similarly, the 4-hydroxytamoxifen-derived drug conjugates

Table 2. Human Estrogen Receptor α Antagonist Activity Determined in a Luciferase Reporter Assay

compound	IC ₅₀ [nM] ^a	CI 95% [nM] ^b
tamoxifen	48.9	26.9–88.7
5a	208.7	107.6–434
5b	100.5	72.0–144.0
5c	11.1	6.2–18.9
5d	232.4	75.5–715.7
5e	6487.0	1693.0–N.D.
7a	335	116.7–N.D.
7b	191.6	131.2–284.5

^aInhibition of receptor activation relative to 10 nM estradiol corresponding to 100% (values represent the mean of at least two independent transfections, SEM typically <15%). ^bCI 95% represents the lower and upper limits of the confidence levels for the IC₅₀ values. N.D. represents not determined, due to lack of convergence. Concentration–response curves are provided as Supporting Information (Figure S1).

14, 17b, 17c, and 17d are 60-, 20-, 2.5-, and 30-fold more potent than the respective non-hydroxylated analogues and **15**, **11**, **11**, and 6-fold more potent than tamoxifen, respectively.

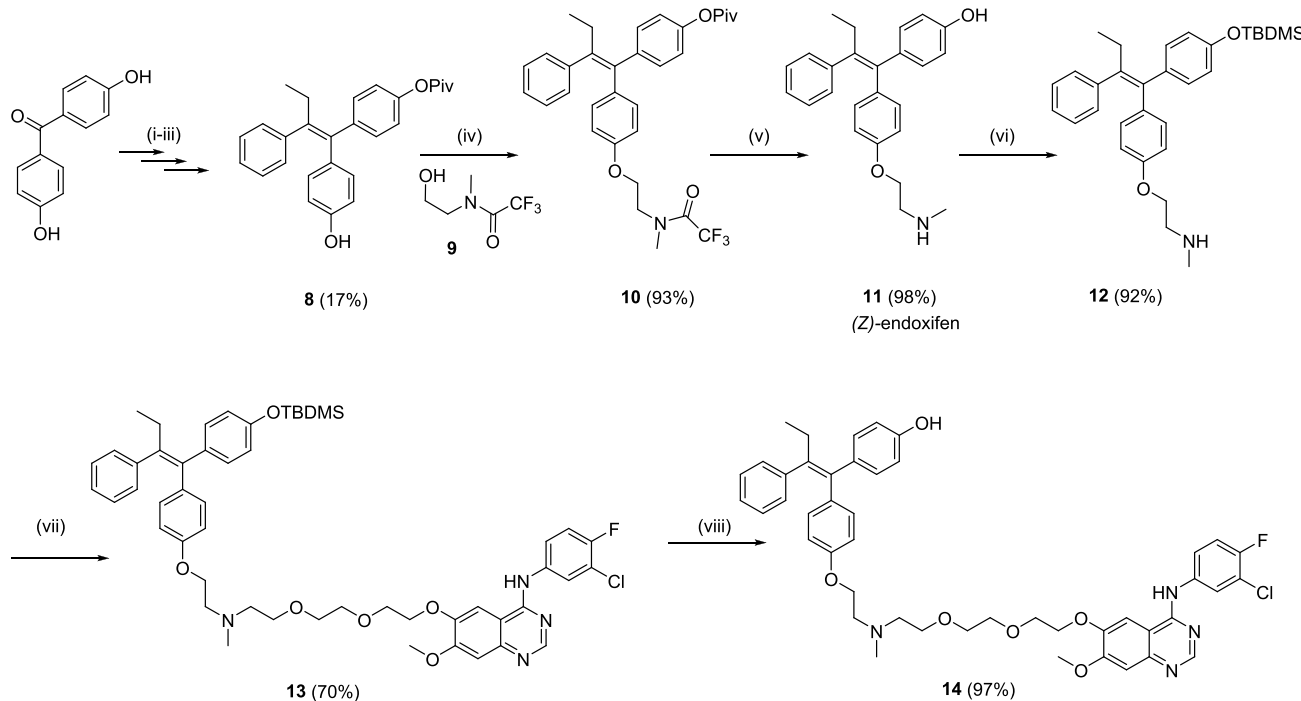
For the hybrid ligands displaying the highest ER α antagonist activity **5c**, **14**, and **17b–d**, their inhibitory activities against wildtype EGFR were determined by a commercially available kinase activity assay (Reaction Biology Hotspot, Malvern, PA, USA) using radiolabeled ³³P(ATP). ^{31,32} The results are summarized in Table 5.

Gefitinib, a highly potent and selective EGFR tyrosine kinase inhibitor with some residual activity on other HER family kinases, acts through competitive ATP displacement from the ATP binding site. Depending on assay conditions, the reported

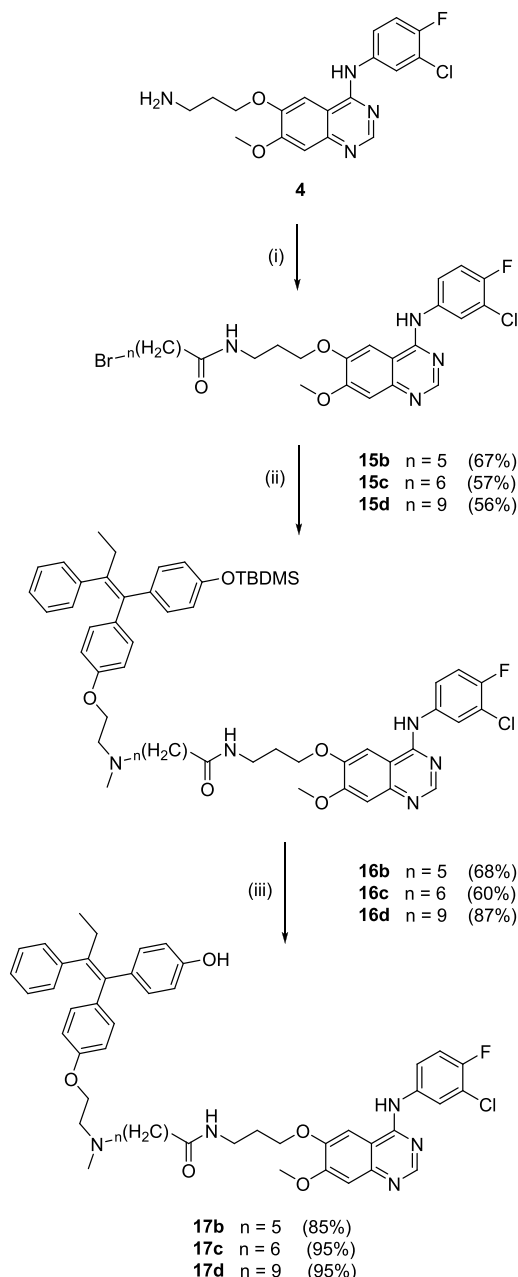
IC₅₀ values range from low nanomolar (33 nM,³³ 15 nM³⁴) to sub-nanomolar (0.51 nM,³⁵ <1 nM)³⁶ concentrations. In the assay employed here, gefitinib demonstrates exceptional potency (IC₅₀ value below 0.1 nM) and thus below the resolution limit of the assay.

The amide-linked hybrid ligands **5c**, **17b**, and **17d** as well as the (PEG)₂-linked analogue **14** exhibit single-digit nanomolar activities (IC₅₀ = 1.1, 2.5, 5.7, and 1.0 nM, respectively) and are significantly more potent than the reference pan-kinase inhibitor staurosporine (IC₅₀ = 16 nM). The similar IC₅₀-values indicate that binding of the gefitinib pharmacophore to the EGFR ATP binding site is not dependent on the length and the chemical constitution of the spacer. Surprisingly, **17c**, the 4-hydroxy analogue of the (CH₂)₆-amide linked hybrid **5c**, demonstrates only moderate potency (IC₅₀ = 261 nM).

Inhibition of Breast Cancer Cell Viability in Phenotypically Diverse Cell Lines. In order to explore how the varied affinities and antagonist potencies for ER α of the hybrid ligands modulate their activity on various types of breast cancer cells, **5b–d** and **17b–d** were screened for their potency and efficacy to inhibit breast cancer cell viability in four phenotypically diverse cell lines: MCF-7 (ER α -positive), MDA-MB-231, MDA-MB-468, and BT-549 (the latter are triple-negative). The MTT assay and XTT assays together with the crystal violet method were used to determine cellular viability at two timepoints, 24 h (MTT assay) and 5 days (XTT assay). The effects of the hybrid compounds on breast cancer cell viability after 5 days of treatment are shown in Figure 3 and Table 6. The concentration–response curves for both 24 h and 5 days treatment are shown in the Supporting information (Figures S3 and S4, respectively). All tested hybrid compounds demonstrate inhibitory activity in the micromolar range with the endoxifen

Scheme 3. Structure and Synthesis of 14^a

^aReagents and conditions: (i) Et₃N, PivCl, THF, 0° to rt; (ii) LiOH·H₂O, 6% MeOH in THF, rt; (iii) propiophenone, Zn, TiCl₄, THF, 0° to reflux, trituration with MeOH; (iv) PPh₃, DIAD, 9, DCM, 0° to rt; (v) LiOH·H₂O, THF/MeOH (5:1), 0° to rt, quant.; (vi) Et₃N, TBDMSCl, DCM, 0° to rt; (vii) Et₃N, **6b**, NMP, 60°; (viii) 1 M Bu₄N⁺F[−] in THF, 0° to rt.

Scheme 4. Structures and Synthesis of 17b–d^a

^aReagents and conditions: (i) $\text{Br}(\text{CH}_2)_n\text{CO}_2\text{H}$, TBTU, DIPEA, DCM, rt; (ii) Et_3N , 12, NMP, 60°; (iii) 1 M $\text{Bu}_4\text{N}^+\text{F}^-$ in THF, 0° to rt.

Table 3. Estrogen Receptor α Binding Assay^b

compound	% inhibition of 0.5 nM [^3H]estradiol binding at a given concentration				
	1 μM	100 nM	10 nM	1 nM	0.1 nM
4-hydroxytamoxifen	N.D.	99.5	99.9	94.3	54.4
endoxifen 11	N.D.	99.8	99.2	77.6	28.9 ^a
14	99.8	90.1	47.3	15.6 ^a	N.D.

^aInhibition lower than 25% is mostly attributable to the variability of the signal around the control level and is not considered significant. N.D.; not determined. ^bValues represent the mean of two independent experiments.

Table 4. Human Estrogen Receptor α Antagonist Activity Determined in a Luciferase Reporter Assay

compound	IC_{50} [nM] ^a	CI 95% [nM] ^b
tamoxifen	48.9	26.9 – 88.7
4-OH-tamoxifen	0.21	0.07 – 0.40
endoxifen 11	0.14	0.048 – 0.17
17b	4.61	2.7 – 7.7
17c	4.4	3.6 – 5.3
17d	7.67	3.13 – 17.0
14	3.2	1.69 – 5.96

^aInhibition of receptor activation relative to 10 nM estradiol corresponding to 100% (values represent the mean of at least two independent transfections, SEM typically <15%). ^bCI 95% represents the lower and upper limits of the confidence levels for the IC_{50} values. Dose-response curves are available as Supporting Information (Figure S1).

Table 5. IC_{50} Values against Wildtype EGFR in a Radiometric Kinase Activity Assay

compound	IC_{50} [nM] ^a	CI 95% [nM] ^b
gefitinib	<0.1 ^c	
staurosporine	16.4	13.1 – 20.45
5c	1.08	0.59 – 2.11
17b	2.51	2.09 – 3.01
17c	260	174.2 – 395
17d	5.72	3.72 – 8.82
14	1.03	0.84 – 1.27

^a IC_{50} values are obtained from duplicate measurements with 10-fold dilution steps starting at 1 or 10 μM , carried out at 1 μM ATP. ^bCI 95% represents the lower and upper limits of the confidence levels for the IC_{50} values. ^c IC_{50} below the resolution limit of the assay. Dose-response curves are available in the Supporting Information (Figure S2).

derivatives being slightly more potent than their tamoxifen counterparts for the BT-549 cell line, while tamoxifen derivatives were more potent against MCF-7 cells. This effect becomes more clear when cells are incubated with these drugs for longer treatment durations (i.e., 5 days vs 24 h) with little or no effect after 24 h treatment (SI, Figure S4). Interestingly, tamoxifen-resistant MCF-7 cell lines¹⁴ display an increase rather than a decrease in proliferation and survival upon compound treatment (Supporting information, Figure S3), which discouraged us from pursuing follow-up studies with longer treatment duration since they became overly confluent.

MCF-7 is a commonly used cell type to investigate breast cancer expressing ER α and initially responding to endocrine therapies, such as tamoxifen.³⁷ For MCF-7 cells, the hybrid ligand pairs with the most favorable overall anticancer profiles were 5b/17b and 5c/17c (with IC_{50} values ranging from 1 to 2 μM , Figure 3 and Table 6). These compounds displayed comparable efficacy to inhibit cell viability and higher potency and efficacy to inhibit cell viability compared to endoxifen alone or endoxifen combined with gefitinib after 5 days of treatment (Figure 3).

Interestingly, treatment of MCF-7 cells with saturating (2 μM) concentrations of our hybrid inhibitors led to differential expression levels of their molecular targets. Specifically, exposure to compounds 17b and 17c induce decreases in expression of ER α , without affecting vinculin expression levels (Figure 4 and Supporting information Figure S5) behaving similar to selective estrogen receptor degraders/downregulators

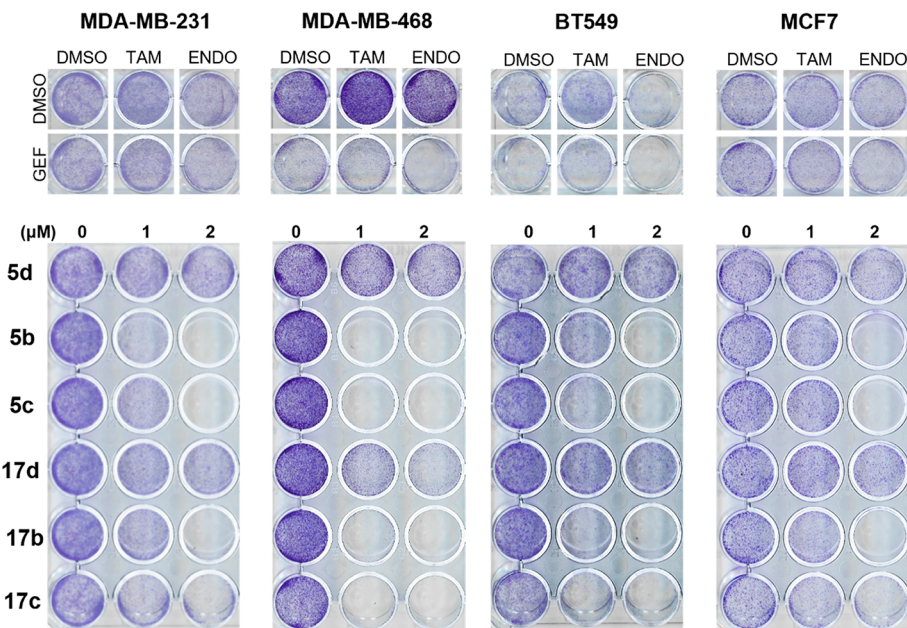


Figure 3. Phenotypically diverse breast cancer cell lines, MDA-MB-231, MDA-MB-468, BT-549 and MCF-7, were exposed to vehicle or the indicated compounds (1 or 2 μ M) for 5 days. Cells were then fixed and stained with crystal violet. Tamoxifen (TAM), endoxifen (ENDO), gefitinib (GEF), and combinations thereof in a 1:1 ratio were used as controls, at the concentration of 5 μ M.

Table 6. IC₅₀ (μ M) Values against Relevant Breast Cancer Cell Lines in the Cell Viability XTT Assay

compound	MDA-MB-231		MDA-MB-468		MCF-7		BT-549	
	IC ₅₀ [μ M] ^a	CI 95% [μ M] ^b	IC ₅₀ [μ M] ^a	CI 95% [μ M] ^b	IC ₅₀ [μ M] ^a	CI 95% [μ M] ^b	IC ₅₀ [μ M] ^a	CI 95% [μ M] ^b
5b	0.78	0.71–0.85	0.69	N.D.	1.19	N.D.	0.60	N.D.–0.82
17b	0.89	0.78–0.98	0.55	N.D.	1.35	N.D.	0.46	0.21–0.55
5c	0.85	0.75–N.D.	0.56	N.D.	1.49	N.D.	0.69	0.51–0.97
17c	0.97	N.D.	0.49	N.D.–0.58	2.00	1.67–3.1	0.38	N.D.–0.54

^aIC₅₀ values (expressed in μ M) are averages from triplicate measurements with 2-fold dilution steps starting at 5 μ M, carried out after 5 days of treatment. ^bCI 95% represent the lower and upper limits of the confidence levels for the IC₅₀ values. N.D. stands for not determined, i.e., where the limit could not be determined within the 95% confidence interval. Concentration–response curves are available in the Supporting Information (Figure S4).

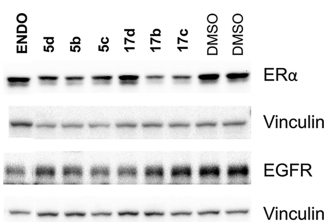


Figure 4. Effect of drug conjugates on expression level of relevant targets, ER α , EGFR, and vinculin, in MCF-7 cells. Cell lysates were prepared from MCF-7 cells exposed to 2 μ M of compounds for 8 h and then subjected to Western blot analysis. See Experimental Section for details. ENDO represents endoxifen.

(SERDs), such as fulvestrant³⁸ and GW76048.³⁹ Indeed, tamoxifen derivatives, with an elongated alkyl tail or changes in the hydrophobic aryl rings, were previously reported to demonstrate SERD activity.^{40–42} As implied by their name, SERDs not only interfere with ER α binding to estradiol but also down-regulate ER α protein levels.

Hasan *et al.* demonstrated that the increased proliferation rate and tamoxifen resistance in TamR-MCF-7 cells arises from constitutive activation of the ER α /ERE (estrogen responsive element) interaction.¹⁴ Given that the SERD mechanism of

action is based on preventing ER dimerization, which causes the ER monomers to be susceptible to proteolytic degradation, we hypothesize that TamR-MCF-7 cell lines would be non-responsive to our hybrid ligands, since ERs would be tightly associated with EREs, therefore preventing the drug conjugates from inducing down-regulation.

Drug conjugates 5b and 5c also performed best with respect to potency for triple-negative BT-549, MDA-MB-468 cells, and MDA-MB-231 cells (IC₅₀ = 560–850 nM) compared to MCF-7 cells (IC₅₀ = 1.19 and 1.49 μ M, respectively) (Table 6). The hydroxylated analogues 17b and 17c also demonstrate high potency to inhibit viability of all three types of TNBC cells (IC₅₀ = 380–970 nM, Table 6) and are less potent at MCF-7 cells (IC₅₀ = 1.35 and 2.0 μ M, respectively). Moreover, at 2 μ M concentration, 5b, 5c, 17b, and 17c show higher or comparable efficacy to inhibit viability of all three types of TNBC cells compared to 5 μ M of the respective controls alone (gefitinib and tamoxifen for 5b and 5c, gefitinib and endoxifen for 17b and 17c), or combinatorial treatment with tamoxifen/endoxifen and gefitinib at 5 μ M each. (Figure 3).

The MDA-MB-231 cells (contain a p53 mutation, KRAS mutation, and wildtype BRCA1) and BT-549 cells (contain PTEN homo deletion, p53 mutation, and wild type BRCA1) are both classified as basal B/claudin-low⁴³ and are epithelial,

adherent, and display a triple-negative hormonal profile. TNBC cell lines although devoid of ER, PR, and HER2 receptors are not the same, but rather heterogeneous in nature.⁴⁴ TNBCs can arise from different mutations (i.e., BRCA, PTEN, and p53) or different levels of receptor expression (i.e., TGF and EGFR).⁴⁵ It is noteworthy that the screened cell lines although reported as triple negative, do in fact express EGFR/ErbB1 (Supporting Information, Figure S6) as shown elsewhere.⁴⁶ Notably, melatonin–tamoxifen drug conjugates displayed anticancer actions in these lines through ER α -independent pathways as previously described.¹⁴

The ER α -independent mechanism of action of tamoxifen on TNBC (MDA-MB-231) and other cancer cell lines (MCF-7) has been demonstrated to occur at low micromolar concentrations.⁴⁶ At such elevated concentrations, tamoxifen, through an inhibition of mitochondrial complex I, increases the ratio of AMP:ATP causing activation of the AMP-activated protein kinase (AMPK) signaling pathway.^{46,47} In cancer cells, the activation of AMPK α 1 results in mTOR-mediated cell death in up to 7 days after treatment. This is consistent with our results that shorter treatments (i.e., 24 h) would provide an incomplete pharmacological picture of our drug conjugates' anti-cancer actions.

In Vitro Metabolic Stability and ADME Properties

Prediction. Five representative hybrid ligands (**5d**, **17b**, **17c**, **17d**, and **14**) were evaluated for their *in vitro* metabolic stability, using mouse liver microsomes (MLM). While the (PEG)₂-linked drug conjugate **14** undergoes significant degradation (ca. 50%) over 2 h incubation, the (CH₂)_n-amide linked compounds demonstrate higher metabolic stability. The non-hydroxylated analogue (**5d**) remains completely intact, while the three hydroxylated ones (**17b**, **17c**, and **17d**) demonstrate only slight degradation (<10%, Figure 5). Mass spectrometric analysis of

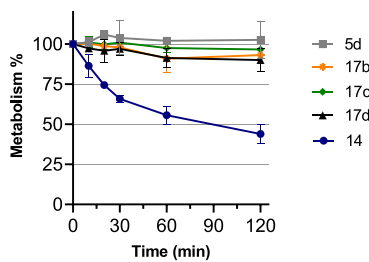


Figure 5. *In vitro* metabolism of compounds **5d**, **17b**, **17c**, **17d**, and **14**. Compound degradation over 120 min incubation time with the mouse liver microsomes is shown. Compound **5d** (gray), compound **17b** (orange), compound **17c** (green), compound **17d** (black), and compound **14** (blue).

the more extensively metabolized compound **14** show that the major metabolic routes could possibly be phase I hydroxylation and *N*- and *O*-dealkylation at different sites of the PEG spacer. For compounds **17b–d**, only hydroxylation could be identified from an *m/z* equaling [M + 17], which indicates that the amide linkage is metabolically stable.

ADME predictions (generated using Schroedinger QikProp, Supporting Information Table S1) suggest that despite the larger molecular weight and polar surface area, the hybrid compounds remain with high predicted oral absorption and skin permeability, with slightly poorer performance on HERG binding (suggesting unspecific binding to this ion channel).

CONCLUSIONS

A series of drug conjugates connecting tamoxifen or its active metabolite endoxifen with the EGFR/HER2-inhibitor gefitinib via a covalent linkage were synthesized and pharmacologically evaluated. While in hybrid ligands **5a–e** and **17b–d**, the pharmacophores are connected by (CH₂)_nCONH-amide groups (*n* = 4–6, 9, and 15), PEG-linkers were used in drug conjugates **7a,b** and **14**. While the amide-linked compounds **5d** and **17 b–d** underwent only minor metabolic transformations, compound **14** with a PEG-spacer showed only moderate metabolic stability in mouse liver microsomes. All hybrid ligands retained both significant ER alpha binding and antagonist activity, as well as EGFR inhibition. The most potent analogues **14**, **17b**, and **17d** exhibit single-digit nanomolar activities at both targets. Moreover, cellular assays assessing cancer cell (MCF-7 and several TNBCs) viability demonstrate that the amide-linked endoxifen-gefitinib drug conjugates **17b** and **17c** are comparable and, at times, superior in their anticancer actions compared to endoxifen, gefitinib, or a combination of both. Most strikingly, **17b** and **17c** display nanomolar IC₅₀ values (380–970 nM) in TNBC cells suggesting an ER-independent mechanism of action. The findings support and underscore the importance for developing novel treatment strategies and therapeutics for the effective treatment of breast cancer.

EXPERIMENTAL SECTION

General Experimental Procedures. All reagents and solvents were purchased from commercial suppliers and were used without further purification. Analytical thin layer chromatography (TLC) was performed using Merck silica gel pre-coated aluminum plates 60 F254 and visualized under a UV lamp at 254 and 366 nm or by means of a suitable staining reagent. Flash column chromatography was carried out on an Interchim PuriFlash 430 automated flash chromatography system using normal phase silica gel Grace Davison Davisil LC60A 20–45 micrometers as stationary phase and Merck Geduran Si60 63–200 micrometers silica for the pre-column. Advion TLC–MS (ESI) with positive/negative modes was used for obtaining the mass spectra. The settings are as follows: ESI voltage 3.50 kV, capillary voltage 187 V, source voltage 44 V, capillary temperature 250 °C, desolvation gas temperature 250 °C, and gas flow 5 L/min nitrogen. HRMS (ESI) for the final compounds was carried out at the MASS Spectrometry Department, Institute of Organic Chemistry, Eberhard-Karls-Universität Tübingen on a Bruker maXis. The instrument settings for the ESI+ mode were as follows: capillary voltage +4500 V, end plate offset –500 V, nebulizer pressure 1.2 bar, dry heater temperature 200 °C, dry gas flow rate 6.0 L/min, and APCI heater temperature 0 °C. The *m/z* scan range was from 80 to 1100 *m/z*. Nuclear magnetic resonance (NMR) spectra were measured using a Bruker Avance 200, Bruker Avance 400, or Bruker Avance 600 MHz. The chemical shifts were calibrated against the residual peak of the deuterated solvent used and were reported in parts per million (ppm) relative to TMS (no internal standard used). The purity of the test compounds was determined via reverse phase high performance liquid chromatography (RP-HPLC) using Phenomenex Luna C8 RP columns (150 × 4.6 mm, 5 μ m) on an Agilent 1100 Series LC with UV diode array detector (DAD) at λ = 254 and 230 nm. The chromatographic separation was performed using the following gradient: 0.01 M KH₂PO₄, pH 2.30 (solvent A), MeOH (solvent B), 40% B to 85% B in 8 min, 85% B for 5 min, 85% to 40% B in 1 min, 40% B for 2 min, stop time 16 min, flow rate 1.5 mL/min and injection volume 5 μ L. All final compounds had a purity of ≥95% confirmed by HPLC at the two different wavelengths. The synthetic procedures and the detailed analytical characterization of the previously reported intermediates **8** and **9** are provided in the Supporting Information.

Synthesis. General Procedure for the Synthesis of Esters 1a–e. Under argon, the indicated amount of NaH (60% dispersion in mineral oil; 1.5 equiv) was added in small portions to a stirred and

cooled solution of *N*-desmethyltamoxifen⁴⁸ in dry DMF (ca. 0.1 M). Stirring was continued for 15 min, and then 1.5 equiv of the corresponding alkylating agent, pre-dissolved in DMF (ca. 0.3 M), was added dropwise to the reaction mixture. The reaction was left to stir overnight at 60 °C. After approximately 80% conversion was reached, the reaction was quenched with saturated NaHCO₃ solution (15 mL) and extracted (5 × 15 mL) using ethyl acetate. The combined organic layers were dried over anhydrous Na₂SO₄, filtered, and concentrated to yield the crude product, which was further purified by gradient flash chromatography using DCM/2 N NH₃ in MeOH (1–5%).

Methyl (Z)-5-((2-(4-(1,2-Diphenylbut-1-en-1-yl)phenoxy)ethyl)-(methyl)amino) Pentanoate (1a). **1a** (274 mg, 83%) was obtained from 250 mg (0.70 mmol) of *N*-desmethyltamoxifen, 205 mg (1.05 mmol) of methyl-5-bromovalerate, and 42 mg (1.05 mmol) of 60% NaH as a colorless oil. ¹H NMR (400 MHz, CDCl₃) δ 7.35 (t, *J* = 7.2 Hz, 2H), 7.29–7.23 (m, 3H), 7.21–7.10 (m, 5H), 6.78 (d, *J* = 8.8 Hz, 2H), 6.55 (d, *J* = 8.8 Hz, 2H), 3.95 (t, *J* = 5.9 Hz, 2H), 3.65 (s, 3H), 2.74 (t, *J* = 5.9 Hz, 2H), 2.46 (q, *J* = 7.6 Hz, 4H), 2.37–2.28 (m, 5H), 1.69–1.59 (m, 2H), 1.56–1.47 (m, 2H), 0.93 (t, *J* = 7.4 Hz, 3H). ¹³C NMR (101 MHz, CDCl₃) δ 174.1, 156.8, 143.9, 142.5, 141.5, 138.4, 135.7, 132.0, 129.8, 129.6, 128.2, 128.0, 126.6, 126.1, 113.5, 65.8, 57.7, 56.1, 51.6, 42.8, 34.0, 29.1, 26.6, 22.9, 13.7. TLC-MS (ESI) *m/z*: 473 [M + H]⁺; HPLC *t_{ret}* = 8.417 min.

Ethyl (Z)-6-((2-(4-(1,2-Diphenylbut-1-en-1-yl)phenoxy)ethyl)-(methyl)amino)hexanoate (1b). **1b** (307 mg, 78%) was obtained from 282 mg (0.79 mmol) of *N*-desmethyltamoxifen, 264 mg (1.18 mmol) of ethyl-6-bromohexanoate, and 47 mg (1.18 mmol) of 60% NaH as a colorless oil. ¹H NMR (400 MHz, CDCl₃) δ 7.34 (t, *J* = 7.8 Hz, 2H), 7.29–7.23 (m, 3H), 7.20–7.08 (m, 5H), 6.76 (d, *J* = 8.8 Hz, 2H), 6.54 (d, *J* = 8.8 Hz, 2H), 4.11 (q, *J* = 7.1 Hz, 2H), 3.93 (t, *J* = 6.0 Hz, 2H), 2.71 (t, *J* = 6.0 Hz, 2H), 2.50–2.38 (m, 4H), 2.33–2.24 (m, 5H), 1.63 (dt, *J* = 15.2, 7.5 Hz, 2H), 1.48 (dt, *J* = 15.1, 7.4 Hz, 2H), 1.35–1.28 (m, 2H), 1.24 (t, *J* = 7.1 Hz, 3H), 0.92 (t, *J* = 7.4 Hz, 3H). ¹³C NMR (101 MHz, CDCl₃) δ 173.9, 156.9, 144.0, 142.6, 141.4, 138.4, 135.7, 132.0, 129.8, 129.6, 128.2, 128.0, 126.6, 126.1, 113.5, 77.5, 77.2, 77.2, 76.8, 65.9, 60.3, 58.1, 56.2, 43.0, 34.4, 29.1, 27.1, 27.0, 25.0, 14.4, 13.7. TLC-MS (ESI) *m/z*: 500.5 [M + H]⁺; HPLC *t_{ret}* = 8.783 min.

Ethyl (Z)-7-((2-(4-(1,2-Diphenylbut-1-en-1-yl)phenoxy)ethyl)-(methyl)amino)heptanoate (1c). **1c** (220 mg, 70%) was obtained from 220 mg (0.62 mmol) of *N*-desmethyltamoxifen, 219 mg (0.92 mmol) of ethyl-7-bromoheptanoate, and 37 mg (0.92 mmol) of 60% NaH as a colorless oil. ¹H NMR (400 MHz, CDCl₃) δ 7.38–7.30 (m, 2H), 7.28–7.22 (m, 3H), 7.20–7.09 (m, 5H), 6.77 (d, *J* = 8.9 Hz, 2H), 6.54 (d, *J* = 8.9 Hz, 2H), 4.11 (q, *J* = 7.1 Hz, 2H), 3.97 (t, *J* = 5.7 Hz, 2H), 2.81–2.70 (m, 2H), 2.45 (q, *J* = 7.4 Hz, 4H), 2.33 (s, 3H), 2.27 (t, *J* = 7.5 Hz, 2H), 1.64–1.46 (m, 4H), 1.34–1.28 (m, 4H), 1.24 (t, *J* = 7.1 Hz, 3H), 0.92 (t, *J* = 7.4 Hz, 3H). ¹³C NMR (101 MHz, CDCl₃) δ 173.9, 156.7, 144.0, 142.6, 141.5, 138.4, 135.8, 132.0, 129.8, 129.6, 128.2, 128.0, 126.7, 126.2, 113.5, 65.6, 60.3, 58.1, 56.1, 42.8, 34.4, 29.1, 27.2, 26.8, 25.0, 14.4, 13.7. TLC-MS (ESI) *m/z*: 514.9 [M + H]⁺; HPLC *t_{ret}* = 8.213 min.

Ethyl (Z)-10-((2-(4-(1,2-Diphenylbut-1-en-1-yl)phenoxy)ethyl)-(methyl)amino)decanoate (1d). **1d** (455 mg, 73%) was obtained from 400 mg (1.12 mmol) of *N*-desmethyltamoxifen, 469 mg (1.68 mmol) of ethyl-10-bromodecanoate, and 67 mg (1.68 mmol) of 60% NaH as a colorless oil. ¹H NMR (300 MHz, CDCl₃) δ 7.39–7.28 (m, 2H), 7.27–7.21 (m, 3H), 7.19–7.09 (m, 5H), 6.76 (d, *J* = 8.7 Hz, 2H), 6.54 (d, *J* = 8.8 Hz, 2H), 4.12 (q, *J* = 7.1 Hz, 2H), 3.94 (t, *J* = 6.0 Hz, 2H), 2.72 (t, *J* = 6.0 Hz, 2H), 2.52–2.35 (m, 4H), 2.31–2.23 (m, 5H), 1.67–1.54 (m, 2H), 1.51–1.40 (m, 2H), 1.30–1.21 (m, 13H), 0.92 (t, *J* = 7.4 Hz, 3H). ¹³C NMR (75 MHz, CDCl₃) δ 174.0, 156.9, 144.0, 142.6, 141.4, 138.4, 135.6, 132.0, 129.8, 129.6, 128.2, 128.0, 126.6, 126.1, 113.5, 65.9, 60.3, 58.4, 56.2, 43.1, 34.5, 29.6, 29.5, 29.3, 29.1, 27.6, 27.3, 25.1, 14.4, 13.7. TLC-MS (ESI) *m/z*: 556.5 [M + H]⁺; HPLC *t_{ret}* = 9.638 min.

Methyl (Z)-16-((2-(4-(1,2-Diphenylbut-1-en-1-yl)phenoxy)ethyl)-(methyl)amino)hexadecanoate (1e). **1e** (510 mg, 81%) was obtained from 360 mg (1.01 mmol) of *N*-desmethyltamoxifen, 528 mg (1.51

mmol) of methyl-16-bromohexadecanoate, and 60 mg (1.51 mmol) of 60% NaH as a colorless oil. ¹H NMR (200 MHz, CDCl₃) δ 7.41–7.29 (m, 2H), 7.28–7.20 (m, 3H), 7.19–7.05 (m, 5H), 6.76 (d, *J* = 8.8 Hz, 2H), 6.54 (d, *J* = 8.7 Hz, 2H), 3.93 (t, *J* = 6.1 Hz, 2H), 3.66 (s, 3H), 2.70 (t, *J* = 6.0 Hz, 2H), 2.46 (dd, *J* = 13.4, 5.9 Hz, 2H), 2.38–2.29 (m, 2H), 2.28 (s, 3H), 1.69–1.54 (m, 2H), 1.51–1.37 (m, 2H), 1.30–1.21 (m, 20H), 0.92 (t, *J* = 7.4 Hz, 3H). ¹³C NMR (50 MHz, CDCl₃) δ 174.50, 174.2, 156.9, 148.3, 143.0, 142.6, 141.4, 140.2, 138.4, 135.6, 132.0, 132.0, 129.9, 129.9, 129.6, 129.6, 128.2, 128.2, 128.0, 128.0, 126.6, 126.1, 113.5, 113.5, 66.0, 58.5, 56.3, 51.6, 43.1, 34.3, 29.8, 29.6, 29.4, 29.3, 27.6, 27.4, 25.1, 13.7. TLC-MS (ESI) *m/z*: 627 [M + H]⁺; HPLC *t_{ret}* = 11.111 min.

General Procedure for the Synthesis of Acids 2a–e. To a cooled solution (ca. 0.08 M) of the ester intermediates **1a–e** in THF/MeOH (1:1), 1 M LiOH aqueous solution (5 equiv) was added dropwise. The mixture was heated to reflux temperature and was left to stir for approximately 1–3 h until TLC indicated complete conversion. The reaction was allowed to cool to rt and was then neutralized using 1 M aqueous HCl solution until reaching pH 6–7. The product was extracted using DCM (5 × 15 mL) and the combined organic layers were dried over anhydrous Na₂SO₄, filtered, and concentrated under reduced pressure to afford the corresponding acid in almost quantitative yield. The crude product, confirmed by TLC-MS and HPLC, was directly used in the next step without any further purification.

(Z)-5-((2-(4-(1,2-Diphenylbut-1-en-1-yl)phenoxy)ethyl)(methyl)amino)pentanoic Acid (2a). **2a** (245 mg, 97%) was obtained from **1a** (260 mg, 0.55 mmol). TLC-MS (ESI) *m/z*: 459 [M + H]⁺; HPLC *t_{ret}* = 8.627 min.

(Z)-6-((2-(4-(1,2-Diphenylbut-1-en-1-yl)phenoxy)ethyl)(methyl)amino)hexanoic Acid (2b). **2b** (279 mg, 98%) was obtained from **1b** (302 mg, 0.60 mmol). TLC-MS (ESI) *m/z*: 472.4 [M + H]⁺; HPLC *t_{ret}* = 8.580 min.

(Z)-7-((2-(4-(1,2-Diphenylbut-1-en-1-yl)phenoxy)ethyl)(methyl)amino)heptanoic Acid (2c). **2c** (190 mg, 98%) was obtained from **1c** (205 mg, 0.40 mmol). TLC-MS (ESI) *m/z*: 486.4 [M + H]⁺; HPLC *t_{ret}* = 8.315 min.

(Z)-10-((2-(4-(1,2-Diphenylbut-1-en-1-yl)phenoxy)ethyl)(methyl)amino)decanoic Acid (2d). **2d** (406 mg, 96%) was obtained from **1d** (445 mg, 0.80 mmol). TLC-MS (ESI) *m/z*: 528.4 [M + H]⁺; HPLC *t_{ret}* = 8.718 min.

(Z)-16-((2-(4-(1,2-Diphenylbut-1-en-1-yl)phenoxy)ethyl)(methyl)amino)hexadecanoic Acid (2e). **2e** (465 mg, 97%) was obtained from **1e** (490 mg, 0.78 mmol). TLC-MS (ESI) *m/z*: 613.1 [M + H]⁺; HPLC *t_{ret}* = 10.387 min.

tert-Butyl(3-((4-(3-chloro-4-fluorophenyl)amino)-7-methoxyquinazolin-6-yl)oxy)propyl Carbamate (3). *tert*-Butyl (3-bromopropyl) carbamate (2.98 g, 12.5 mmol, 1.6 equiv) was added to a suspension of 4-((3-chloro-4-fluorophenyl)amino)-7-methoxy-quinazolin-6-ol (2.50 g, 7.81 mmol) and K₂CO₃ (3.24 g, 23.44 mmol, 3 equiv) in dry MeCN (20 mL). The reaction mixture was heated up to 70 °C and left to stir overnight. Upon almost complete conversion, the mixture was quenched with saturated solution of NH₄Cl (15 mL) and subsequently extracted using ethyl acetate (5 × 15 mL). The combined organic layers were dried over anhydrous Na₂SO₄, filtered, and concentrated under reduced pressure. The residue was purified by gradient flash chromatography using DCM/2 N NH₃ in MeOH (1–7%) to afford the title compound **3**. Yield: 2.24 g (60%). ¹H NMR (200 MHz, DMSO-*d*₆) δ 9.54 (s, 1H), 8.49 (s, 1H), 8.11 (dd, *J* = 6.8, 2.3 Hz, 1H), 7.87–7.73 (m, 2H), 7.44 (t, *J* = 9.1 Hz, 1H), 7.19 (s, 1H), 6.94 (t, *J* = 5.5 Hz, 1H), 4.15 (t, *J* = 5.3 Hz, 2H), 3.94 (s, 3H), 3.26–3.06 (m, 2H), 2.05–1.86 (m, 2H), 1.37 (s, 9H). ¹³C NMR (50 MHz, DMSO-*d*₆) δ 156.0, 155.7, 154.5, 154.3, 152.6, 148.3, 147.0, 136.9 (d, *J* = 2.8 Hz), 123.4, 122.3 (d, *J* = 6.9 Hz), 118.8 (d, *J* = 18.2 Hz), 116.5 (d, *J* = 21.7 Hz), 108.8, 107.2, 102.5, 77.6, 66.6, 55.9, 37.3, 29.0, 28.3. TLC-MS (ESI) *m/z*: 499.4 [M + Na]⁺; HPLC *t_{ret}* = 7.465 min.

6-(3-Aminopropoxy)-N-(3-chloro-4-fluorophenyl)-7-methoxyquinazolin-4-amine (4). Intermediate **3** (0.50 g, 1.05 mmol) was dissolved in DCM (20 mL). Trifluoroacetic acid (20% v/v) was added dropwise to the ice-cooled stirring solution. The cooling bath was removed, and

the solution was left to stir at ambient temperature until TLC indicated complete conversion (0.5–1 h). The crude product was then basified by dropwise addition of a saturated aqueous solution of NaHCO₃ and extracted using DCM (5 × 15 mL). The combined organic layers were dried over anhydrous Na₂SO₄, filtered, concentrated, and dried in vacuum to yield 98% (384 mg) of the desired amine 4 as a pale yellow solid. The crude material was used as such in the next step without any further purification. ¹H NMR (400 MHz, DMSO-*d*₆) δ 9.57 (s, 1H), 8.49 (s, 1H), 8.12 (dd, *J* = 6.8, 2.6 Hz, 1H), 7.85–7.74 (m, 2H), 7.43 (t, *J* = 9.1 Hz, 1H), 7.19 (s, 1H), 4.21 (t, *J* = 6.3 Hz, 2H), 3.94 (s, 3H), 2.78 (t, *J* = 6.5 Hz, 2H), 1.97–1.85 (m, 2H). ¹³C NMR (101 MHz, DMSO-*d*₆) δ 156.5, 155.0, 153.6 (d, *J* = 242.7 Hz), 153.0, 148.9, 147.4, 137.3 (d, *J* = 2.7 Hz), 123.9, 122.8 (d, *J* = 6.8 Hz), 119.2 (d, *J* = 18.4 Hz), 117.0 (d, *J* = 21.7 Hz), 109.3, 107.7, 102.9, 67.3, 56.3, 40.6, 40.4, 40.2, 40.0, 39.8, 39.6, 39.4, 38.8, 32.6. TLC-MS (ESI) *m/z*: 377.2 [M + H]⁺; HPLC *t*_{ret} = 1.455 min.

General Procedure for the Synthesis of 5a–e. To a stirred solution of the crude acid (1.05 equiv) dissolved in dry DMF (ca. 0.06 M), TBTU (1.5 equiv) was added portionwise, and the reaction was left to stir for 10–15 min. DIPEA (3 equiv) and the amine 4 dissolved in DMF were then added dropwise and stirring at room temperature was continued until HPLC indicated full consumption of the reacting amine (1–2 h). A saturated aqueous solution of NH₄Cl (20 mL) was added, and the aqueous layer was extracted with ethyl acetate (3 × 20 mL). The combined organic layers were washed with saturated aqueous NaHCO₃ solution and brine (20 mL each), dried over anhydrous Na₂SO₄, and concentrated under reduced pressure. Purification of the crude residue was carried out via flash chromatography to obtain the hybrid ligands 5a–e.

(Z)-N-(3-((4-((3-Chloro-4-fluorophenyl)amino)-7-methoxyquinazolin-6-yl)oxy)propyl)-5-((2-(4-(1,2-diphenylbut-1-en-1-yl)-phenoxyethyl)(methyl)amino)pentanamide (**5a**). **5a** (77 mg, 39%) was obtained from amine 4 (91 mg, 0.24 mmol), **2a** (115 mg, 0.25 mmol), TBTU (116 mg, 0.36 mmol) and DIPEA (125 μL, 0.72 mmol) after gradient flash chromatography purification using EtOAc/2 N NH₃ in MeOH (1–6%) as colorless oil. ¹H NMR (400 MHz, CDCl₃) δ 8.86 (s, 1H), 8.68 (s, 1H), 8.06 (dd, *J* = 6.6, 2.4 Hz, 1H), 7.87–7.80 (m, 1H), 7.76 (s, 1H), 7.38 (t, *J* = 7.3 Hz, 2H), 7.34–7.26 (m, 4H), 7.22–7.11 (m, 6H), 6.80 (d, *J* = 8.7 Hz, 2H), 6.62 (t, *J* = 5.3 Hz, 1H), 6.58–6.50 (m, 2H), 4.19 (t, *J* = 6.3 Hz, 2H), 4.01 (s, 3H), 3.92 (t, *J* = 5.5 Hz, 2H), 3.52–3.44 (m, 2H), 2.70 (t, *J* = 5.5 Hz, 2H), 2.49 (q, *J* = 7.4 Hz, 2H), 2.39 (t, *J* = 6.9 Hz, 2H), 2.30–2.22 (m, 5H), 2.10–2.05 (m, 2H), 1.70–1.61 (m, 2H), 1.54–1.45 (m, 2H), 0.96 (t, *J* = 7.4 Hz, 3H). ¹³C NMR (101 MHz, CDCl₃) δ 174.3, 156.9, 156.8, 154.6 (d, *J* = 245.3 Hz), 155.6, 153.9, 148.1, 148.0, 143.9, 142.6, 141.7, 138.36, 136.42 (d, *J* = 3.1 Hz), 136.0, 132.0, 129.8, 129.6, 128.3, 128.0, 126.7, 126.2, 124.0, 121.7 (d, *J* = 7.0 Hz), 120.8 (d, *J* = 18.7 Hz), 116.4 (d, *J* = 21.9 Hz), 113.5, 109.6, 108.1, 105.3, 68.6, 65.7, 57.6, 56.4, 56.3, 42.7, 37.4, 36.6, 29.8, 28.9, 26.6, 23.9, 13.7. TLC-MS (ESI) *m/z*: 838.9 [M + Na]⁺; HRMS (ESI): calcd for C₄₈H₅₁ClFN₅O₄ [M + H]⁺ 816.36136, found 816.36857; HPLC *t*_{ret} = 8.678 min.

(Z)-N-(3-((4-((3-Chloro-4-fluorophenyl)amino)-7-methoxyquinazolin-6-yl)oxy)propyl)-6-((2-(4-(1,2-diphenylbut-1-en-1-yl)-phenoxyethyl)(methyl)amino)hexanamide (**5b**). **5b** (81 mg, 42%) was obtained from amine 4 (87 mg, 0.23 mmol), **2b** (114 mg, 0.24 mmol), TBTU (89 mg, 0.35 mmol) and DIPEA (121 μL, 0.69 mmol) after gradient flash chromatography purification using EtOAc/2 N NH₃ in MeOH (1–4%) as colorless oil. ¹H NMR (400 MHz, DMSO-*d*₆) δ 9.54 (s, 1H), 8.50 (s, 1H), 8.12 (dd, *J* = 6.8, 2.5 Hz, 1H), 7.88 (t, *J* = 5.4 Hz, 1H), 7.83–7.78 (m, 2H), 7.43 (t, *J* = 9.1 Hz, 1H), 7.36 (t, *J* = 7.4 Hz, 2H), 7.26 (t, *J* = 7.3 Hz, 1H), 7.22–7.14 (m, 5H), 7.10 (t, *J* = 5.8 Hz, 3H), 6.69 (d, *J* = 8.7 Hz, 2H), 6.56 (d, *J* = 8.7 Hz, 2H), 4.16 (t, *J* = 5.9 Hz, 2H), 3.93 (s, 3H), 3.83 (t, *J* = 5.8 Hz, 2H), 3.25 (dd, *J* = 12.2, 6.4 Hz, 2H), 2.54 (t, *J* = 5.8 Hz, 2H), 2.34 (q, *J* = 7.3 Hz, 2H), 2.25 (t, *J* = 7.1 Hz, 2H), 2.11 (s, 3H), 2.04 (t, *J* = 7.3 Hz, 2H), 1.99–1.92 (m, 2H), 1.51–1.41 (m, 2H), 1.38–1.30 (m, 2H), 1.24–1.16 (m, 2H), 0.82 (t, *J* = 7.4 Hz, 3H). ¹³C NMR (101 MHz, DMSO-*d*₆) δ 172.2, 156.4, 156.0, 154.5, 153.1 (d, *J* = 242.7 Hz), 152.6, 148.3, 147.0, 143.3, 141.8, 140.7, 137.9, 136.8 (d, *J* = 2.9 Hz), 134.8, 131.3, 129.3, 128.9, 128.3, 127.9, 126.6, 126.1, 123.4, 122.2 (d, *J* = 6.8 Hz), 118.8 (d, *J* = 18.3 Hz), 116.4 (d, *J* = 21.5 Hz), 113.5, 108.8, 107.3, 102.6, 66.7, 65.7, 57.4, 55.9, 55.7, 42.4, 35.6, 35.5, 28.9, 28.8, 28.7, 28.5, 26.8, 26.7, 25.3, 13.3. TLC-MS (ESI) *m/z*: 886.7 [M + H]⁺; HRMS (ESI): calcd for C₅₃H₆₁ClFN₅O₄ [M + H]⁺ 886.43961, found 886.44752; HPLC *t*_{ret} = 9.182 min.

(Z)-N-(3-((4-((3-Chloro-4-fluorophenyl)amino)-7-methoxyquinazolin-6-yl)oxy)propyl)-7-((2-(4-(1,2-diphenylbut-1-en-1-yl)-phenoxyethyl)(methyl)amino)heptanamide (**5c**). **5c** (90 mg, 44%) was obtained from amine 4 (91 mg, 0.24 mmol), **2c** (124 mg, 0.25 mmol), TBTU (116 mg, 0.36 mmol) and DIPEA (126 μL, 0.72 mmol) after gradient flash chromatography purification using EtOAc/2 N NH₃ in MeOH (1–5%) as colorless oil. ¹H NMR (400 MHz, DMSO-*d*₆) δ 9.54 (s, 1H), 8.50 (s, 1H), 8.12 (dd, *J* = 6.8, 2.6 Hz, 1H), 7.87 (t, *J* = 5.4 Hz, 1H), 7.83–7.77 (m, 2H), 7.43 (t, *J* = 9.1 Hz, 1H), 7.39–7.33 (m, 2H), 7.30–7.24 (m, 1H), 7.21 (s, 1H), 7.20–7.14 (m, 4H), 7.13–7.07 (m, 3H), 6.70 (d, *J* = 8.7 Hz, 2H), 6.56 (d, *J* = 8.8 Hz, 2H), 4.16 (t, *J* = 6.0 Hz, 2H), 3.93 (s, 3H), 3.84 (t, *J* = 5.9 Hz, 2H), 3.25 (dd, *J* = 12.4, 6.5 Hz, 2H), 2.54 (t, *J* = 5.9 Hz, 2H), 2.35 (q, *J* = 7.3 Hz, 2H), 2.27–2.21 (m, 2H), 2.11 (s, 3H), 2.04 (t, *J* = 7.4 Hz, 2H), 2.00–1.91 (m, 2H), 1.49–1.40 (m, 2H), 1.36–1.26 (m, 2H), 1.23–1.15 (m, 4H), 0.83 (t, *J* = 7.4 Hz, 3H). ¹³C NMR (101 MHz, DMSO-*d*₆) δ 172.2, 156.4, 156.0, 154.5, 153.1 (d, *J* = 242.7 Hz), 152.7, 148.3, 147.0, 143.3, 141.8, 140.7, 137.9, 136.8 (d, *J* = 3.1 Hz), 134.8, 131.3, 129.3, 128.9, 128.3, 127.9, 126.6, 126.2, 123.4, 122.2 (d, *J* = 6.7 Hz), 118.8 (d, *J* = 18.3 Hz), 116.5 (d, *J* = 21.5 Hz), 113.4, 108.8, 107.3, 102.6, 66.63, 65.62, 57.3, 55.9, 55.7, 42.3, 35.6, 35.4, 28.8, 28.6, 28.5, 26.58, 26.55, 25.3, 13.3. TLC-MS (ESI) *m/z*: 844.5 [M + H]⁺; HRMS (ESI): calcd for C₅₀H₅₅ClFN₅O₄ [M + H]⁺ 844.39266, found 844.39968; HPLC *t*_{ret} = 8.669 min.

(Z)-N-(3-((4-((3-Chloro-4-fluorophenyl)amino)-7-methoxyquinazolin-6-yl)oxy)propyl)-10-((2-(4-(1,2-diphenylbut-1-en-1-yl)-phenoxyethyl)(methyl)amino)decanamide (**5d**). **5d** (40 mg, 24%) was obtained from amine 4 (70 mg, 0.19 mmol), **2d** (103 mg, 0.20 mmol), TBTU (89 mg, 0.28 mmol), and DIPEA (97 μL, 0.56 mmol) after gradient flash chromatography purification using DCM/2 N NH₃ in MeOH (1–8%) as colorless oil. ¹H NMR (400 MHz, DMSO-*d*₆) δ 9.54 (s, 1H), 8.49 (s, 1H), 8.12 (dd, *J* = 6.7, 2.2 Hz, 1H), 7.87 (t, *J* = 5.0 Hz, 1H), 7.84–7.76 (m, 2H), 7.39 (dt, *J* = 14.8, 8.3 Hz, 3H), 7.27 (t, *J* = 7.3 Hz, 1H), 7.23–7.08 (m, 8H), 6.70 (d, *J* = 8.5 Hz, 2H), 6.56 (d, *J* = 8.6 Hz, 3H), 4.16 (t, *J* = 5.6 Hz, 2H), 3.93 (s, 3H), 3.85 (t, *J* = 5.7 Hz, 2H), 3.26 (dd, *J* = 11.6, 5.9 Hz, 2H), 2.55 (t, *J* = 5.6 Hz, 2H), 2.35 (dd, *J* = 14.5, 7.1 Hz, 2H), 2.24 (t, *J* = 7.1 Hz, 2H), 2.12 (s, 3H), 2.04 (t, *J* = 7.2 Hz, 2H), 1.99–1.90 (m, 2H), 1.51–1.39 (m, 2H), 1.32–1.24 (m, 2H), 1.22–1.12 (m, 10H), 0.83 (t, *J* = 7.3 Hz, 3H). ¹³C NMR (101 MHz, DMSO-*d*₆) δ 172.3, 156.5, 156.0, 154.6, 153.2 (d, *J* = 242.7 Hz), 152.7, 148.3, 147.0, 143.3, 141.8, 140.7, 137.9, 136.9 (d, *J* = 2.4 Hz), 134.8, 131.3, 129.4, 128.9, 128.3, 127.9, 126.7, 126.2, 123.4, 122.2 (d, *J* = 6.8 Hz), 118.8 (d, *J* = 18.3 Hz), 116.5 (d, *J* = 21.5 Hz), 113.5, 108.8, 107.3, 102.6, 66.7, 65.7, 57.4, 55.9, 55.7, 42.4, 35.6, 35.5, 28.9, 28.8, 28.7, 28.5, 26.8, 26.7, 25.3, 13.3. TLC-MS (ESI) *m/z*: 886.7 [M + H]⁺; HRMS (ESI): calcd for C₅₅H₆₁ClFN₅O₄ [M + H]⁺ 886.43961, found 886.44752; HPLC *t*_{ret} = 9.182 min.

(Z)-N-(3-((4-((3-Chloro-4-fluorophenyl)amino)-7-methoxyquinazolin-6-yl)oxy)propyl)-16-((2-(4-(1,2-diphenylbut-1-en-1-yl)-phenoxyethyl)(methyl)amino)hexadecanamide (**5e**). **5e** (71 mg, 51%) was obtained from amine 4 (54 mg, 0.14 mmol), **2e** (90 mg, 0.15 mmol), TBTU (69 mg, 0.21 mmol), and DIPEA (74 μL, 0.43 mmol) after gradient flash chromatography purification using DCM/2 N NH₃ in MeOH (1–8%) as colorless oil. ¹H NMR (400 MHz, CDCl₃) δ 8.68 (s, 1H), 8.65 (s, 1H), 8.03 (dd, *J* = 6.6, 2.6 Hz, 1H), 7.78 (ddd, *J* = 8.9, 4.1, 2.7 Hz, 1H), 7.68 (s, 1H), 7.36–7.31 (m, 2H), 7.28–7.21 (m, 5H), 7.19–7.09 (m, 6H), 6.76 (d, *J* = 8.8 Hz, 2H), 6.53 (d, *J* = 8.9 Hz, 2H), 4.19 (t, *J* = 6.2 Hz, 2H), 3.98 (s, 3H), 3.93 (t, *J* = 6.0 Hz, 2H), 3.56–3.47 (m, 2H), 2.72 (t, *J* = 6.0 Hz, 2H), 2.48–2.42 (m, 2H), 2.42–2.37 (m, 2H), 2.29 (s, 3H), 2.23–2.16 (m, 2H), 2.12–2.05 (m, 2H), 1.63–1.54 (m, 2H), 1.49–1.40 (m, 2H), 1.26–1.17 (m, 2H), 0.91 (t, *J* = 7.4 Hz, 3H). ¹³C NMR (101 MHz, CDCl₃) δ 174.4, 156.8, 155.4, 154.6 (d, *J* = 245.4 Hz), 153.9, 148.1, 147.9, 143.9, 142.6, 141.5, 138.4, 136.2 (d, *J* = 2.9 Hz), 135.7, 132.0, 129.8, 129.6, 128.2, 128.0, 126.6, 126.1, 124.0, 121.7 (d, *J* = 6.6 Hz), 120.8 (d, *J* = 18.6 Hz), 116.4 (d, *J* = 21.8 Hz), 113.5, 109.5, 108.0, 104.7, 68.6, 65.8, 58.4, 56.3, 56.2, 43.0, 37.5, 37.2, 29.7, 29.6, 29.5, 29.4, 29.1, 28.9, 27.6, 27.2, 26.0, 13.7. TLC-MS (ESI)

m/z: 970.7 [M + H]⁺; HRMS (ESI): exact mass calcd for C₅₉H₇₃ClFN₅O₄ [M + H]⁺ 970.53351, found 970.53940; HPLC *t_{ret}* = 10.098 min.

General Procedure for the Synthesis of Compounds 6a – b.

An ice cooled suspension of *O*-desmorpholinopropyl gefitinib in dry DMF (ca. 0.06 M) under argon was treated with small portions of NaH (60% dispersion in mineral oil; 1 equiv). After stirring for 15 min, the corresponding alkylating agent (4 equiv) dissolved in dry DMF (ca. 1.2 M) was added dropwise and then the reaction was allowed to stir until the TLC indicated full consumption of the *O*-desmorpholinopropyl gefitinib (~4 h). Upon completion, the reaction was quenched with brine (15 mL) and extracted using ethyl acetate (3 × 15 mL). The combined organic layers were dried over anhydrous Na₂SO₄, filtered, evaporated under reduced pressure, and purified by flash chromatography to yield compounds 6a,b.

N-(3-Chloro-4-fluorophenyl)-6-(2-(2-iodoethoxy)ethoxy)-7-methoxyquinazolin-4-amine (6a). 6a (105 mg, 65%) was obtained from 100 mg (0.31 mmol) of *O*-desmorpholinopropyl gefitinib, 408 mg (1.24 mmol) of 1-iodo-2-(2-iodoethoxy)ethane, and 12 mg (0.31 mmol) of 60% NaH after gradient flash chromatography purification using DCM/2 N NH₃ in MeOH (1–7%) as colorless oil. ¹H NMR (200 MHz, CDCl₃) δ 8.71 (s, 1H), 8.11 (s, 1H), 7.97 (d, *J* = 5.2 Hz, 1H), 7.74–7.54 (m, 2H), 7.31–7.09 (m, 2H), 4.35 (*t*, *J* = 6.2 Hz, 2H), 4.01 (s, 3H), 3.98–3.84 (m, 4H), 3.35 (*t*, *J* = 6.3 Hz, 2H). ¹³C NMR (101 MHz, CDCl₃) δ 157.0, 155.9, 153.6, 153.5, 153.4, 148.7, 147.6, 143.8, 142.5, 141.8, 138.1, 136.4, 136.1, 132.1, 129.8, 129.5, 128.3, 128.0, 126.7, 126.2, 124.4, 122.0 (d, *J* = 6.6 Hz), 120.8 (d, *J* = 17.6 Hz), 116.4 (d, *J* = 21.5 Hz), 113.4, 109.4, 107.5, 104.1, 69.5, 68.9, 56.9, 56.6, 55.7, 42.2, 29.2, 13.7. TLC-MS (ESI) *m/z:* 518.1 [M + H]⁺; HPLC *t_{ret}* = 7.101 min.

N-(3-Chloro-4-fluorophenyl)-6-(2-(2-iodoethoxy)ethoxy)-ethoxy)-7-methoxyquinazolin-4-amine (6b). 6b (270 mg, 78%) was obtained from 200 mg (0.63 mmol) of *O*-desmorpholinopropyl gefitinib, 926 mg (2.50 mmol) of 1,2-bis(2-iodoethoxy)ethane, and 25 mg (0.63 mmol) of 60% NaH after gradient flash chromatography purification using DCM/2 N NH₃ in MeOH (1–5%) as colorless oil. ¹H NMR (400 MHz, DMSO-*d*₆) δ 9.54 (s, 1H), 8.50 (s, 1H), 8.11 (dd, *J* = 6.8, 2.6 Hz, 1H), 7.85–7.74 (m, 2H), 7.45 (*t*, *J* = 9.1 Hz, 1H), 7.21 (s, 1H), 4.33–4.25 (m, 2H), 3.94 (s, 3H), 3.91–3.86 (m, 2H), 3.70–3.64 (m, 4H), 3.63–3.59 (m, 2H), 3.31 (*t*, *J* = 6.4 Hz, 2H). ¹³C NMR (101 MHz, DMSO-*d*₆) δ 155.7, 154.3, 153.0 (d, *J* = 242.7 Hz), 152.5, 148.0, 146.8, 136.6 (d, *J* = 3.0 Hz), 123.3, 122.1 (d, *J* = 6.7 Hz), 118.6 (d, *J* = 18.5 Hz), 116.4 (d, *J* = 21.7 Hz), 108.5, 107.1, 102.4, 70.8, 69.8, 69.2, 68.5, 68.1, 55.7, 5.2. TLC-MS (ESI) *m/z:* 562.7 [M + H]⁺; HPLC *t_{ret}* = 8.709 min.

General Procedure for the Synthesis of Compounds 7a,b.

The indicated amount of NaH (60% dispersion in mineral oil; 2 equiv) was added portionwise to a stirring solution of *N*-desmethyltamoxifen (1.1 equiv) in dry DMF (ca. 0.05 M) under an argon atmosphere. After 10–15 min, 6a or 6b dissolved in dry DMF (ca. 0.1 M) was added dropwise to the deprotonated amine and stirring was continued overnight. The reaction was then quenched with saturated aqueous NH₄Cl solution (15 mL) and extracted with EtOAc (3 × 15 mL). The organic layer was subsequently washed with brine (3 × 15 mL), dried over anhydrous Na₂SO₄, and evaporated under reduced pressure. The crude product was purified using flash chromatography to obtain 7a,b.

(Z)-N-(3-Chloro-4-fluorophenyl)-6-(2-(2-(2-(4-(1,2-diphenylbut-1-en-1-yl)phenoxy)ethyl)(methyl)amino)ethoxy)ethoxy)-7-methoxyquinazolin-4-amine (7a). 7a (52 mg, 30%) was obtained from 120 mg (0.23 mmol) of 6a, 90 mg (0.25 mmol) of *N*-desmethyltamoxifen and 18 mg (0.46 mmol) of 60% NaH after gradient flash chromatography purification using EtOAc/2 N in NH₃ MeOH (1–7%) as colorless oil. ¹H NMR (200 MHz, CDCl₃) δ 8.63 (s, 1H), 7.92 (dd, *J* = 6.3, 1.9 Hz, 1H), 7.83 (s, 1H), 7.60–7.51 (m, 1H), 7.45 (s, 1H), 7.35–7.29 (m, 2H), 7.25–7.01 (m, 10H), 6.74 (d, *J* = 8.5 Hz, 2H), 6.48 (d, *J* = 8.5 Hz, 2H), 4.37–4.26 (m, 2H), 3.99–3.81 (m, 7H), 3.70 (*t*, *J* = 5.7 Hz, 2H), 2.84 (*t*, *J* = 4.3 Hz, 2H), 2.79–2.70 (m, 2H), 2.50–2.38 (m, 2H), 2.36 (s, 3H), 0.94–0.87 (m, 3H). ¹³C NMR (101 MHz, CDCl₃) δ 157.0, 155.9, 153.6, 153.5, 153.4, 148.7, 147.6, 143.8, 142.5, 141.8, 138.1, 136.4, 136.1, 132.1, 129.8, 129.5, 128.3, 128.0, 126.7,

126.2, 124.4, 122.0 (d, *J* = 6.6 Hz), 120.8 (d, *J* = 17.6 Hz), 116.4 (d, *J* = 21.5 Hz), 113.4, 109.4, 107.5, 104.1, 69.5, 68.9, 56.9, 56.6, 55.7, 42.2, 29.2, 13.7. TLC-MS (ESI) *m/z:* 747.9 [M + H]⁺; HRMS (ESI): calcd for C₄₄H₄₄ClFN₄O₄ [M + H]⁺ 747.30351, found 747.31182; HPLC *t_{ret}* = 9.064 min.

(Z)-N-(3-Chloro-4-fluorophenyl)-6-(2-(2-(2-(4-(1,2-diphenylbut-1-en-1-yl)phenoxy)ethyl)(methyl)amino)ethoxy)ethoxy)-ethoxy)-7-methoxyquinazolin-4-amine (7b). 7b (84 mg, 38%) was obtained from 160 mg (0.28 mmol) of 6b, 110 mg (0.31 mmol) of *N*-desmethyltamoxifen, and 22 mg (0.56 mmol) of 60% NaH after gradient flash chromatography purification using DCM/2 N NH₃ in MeOH (1–7%) as colorless oil. ¹H NMR (400 MHz, CDCl₃) δ 8.61 (s, 1H), 8.39 (s, 1H), 7.99–7.89 (m, 1H), 7.68 (s, 1H), 7.65–7.59 (m, 1H), 7.33 (*t*, *J* = 7.3 Hz, 2H), 7.23–7.04 (m, 10H), 6.72 (d, *J* = 8.8 Hz, 2H), 6.44 (d, *J* = 8.8 Hz, 2H), 4.42 (*t*, *J* = 5.1 Hz, 2H), 3.97 (s, 3H), 3.89 (*t*, *J* = 5.1 Hz, 4H), 3.72–3.69 (m, 2H), 3.66–3.60 (m, 4H), 2.83–2.66 (m, 4H), 2.43 (*q*, *J* = 7.4 Hz, 2H), 2.31 (s, 3H), 0.91 (*t*, *J* = 7.4 Hz, 3H). ¹³C NMR (101 MHz, CDCl₃) δ 156.8, 155.4, 153.8, 148.7, 147.9, 143.9, 142.5, 141.7, 138.2, 136.0, 132.0, 129.8, 129.6, 128.3, 128.0, 126.7, 126.2, 124.5, 122.3 (d, *J* = 7.7 Hz), 116.5 (d, *J* = 22.1 Hz), 113.4, 109.4, 108.0, 104.1, 70.7, 70.1, 69.8, 69.3, 57.2, 56.4, 56.3, 42.9, 29.2, 13.7. TLC-MS (ESI) *m/z:* 792.0 [M + H]⁺; HRMS (ESI): calcd for C₄₆H₄₈ClFN₄O₅ [M + Na]⁺ 813.32973, found 813.31952; HPLC *t_{ret}* = 8.794 min.

(E)-4-(2-Phenyl-1-(4-(2-(2,2,2-trifluoro-N-methylacetamido)ethoxy)phenyl)but-1-en-1-yl)phenyl Pivalate (10). 8 (250 mg, 0.62 mmol), 9 (320 mg, 1.87 mmol, 3 equiv) and triphenylphosphine (PPh₃; 1.64 g, 6.24 mmol, 10 equiv) were dissolved in dry DCM (3 mL) in a Schlenk flask under argon. The solution was cooled in an ice bath and then treated dropwise with an excess of diisopropylazodicarboxylate (DIAD; 1.26 g, 6.24 mmol, 10 equiv) dissolved in anhydrous DCM (5 mL) before leaving it to stir at rt overnight. Only using 10 equiv of both DIAD and PPh₃ made the reaction proceed to completion with almost total conversion monitored by TLC and HPLC. The solvent was evaporated, and the product was directly purified by gradient flash chromatography using 100% hexane to Hex:DCM:EtOAc (3:1:1) to afford 321 mg (93%) as a white solid. ¹H NMR (400 MHz, CDCl₃) δ 7.20–6.94 (m, 10H), 6.70 (d, *J* = 8.8 Hz, 2H), 6.44 (d, *J* = 8.8 Hz, 2H), 4.01–3.91 (m, 2H), 3.70–3.65 (m, 2H), 3.18–3.15 (m, 3.09–3.00 (m, 3H), 2.39 (*q*, *J* = 7.4 Hz, 2H), 1.29 (s, 9H), 0.84 (*t*, *J* = 7.4 Hz, 3H). ¹³C NMR (101 MHz, CDCl₃) δ 177.3, 156.3, 156.1, 149.9, 142.4, 142.2, 141.2, 137.3, 136.1, 132.2, 130.5, 129.8, 128.1, 126.3, 121.3, 114.5 (m), 113.4, 66.2, 65.6, 49.7, 48.9 (*q*, *J* = 3.5 Hz), 39.3, 37.2 (m), 36.2, 29.2, 27.3, 13.7. TLC-MS (ESI) *m/z:* 576.7 [M + Na]⁺; HPLC *t_{ret}* = 13.754 min.

(Z)-4-(1-(4-(2-(Methylamino)ethoxy)phenyl)-2-phenylbut-1-en-1-yl)phenol (11). To an ice-cooled solution of 10 (300 mg, 0.54 mmol) in 10 mL of THF/MeOH (5:1), LiOH·H₂O (5 equiv) was added portionwise. The ice bath was removed, and the reaction was left to stir at rt until TLC indicated complete deprotection. The reaction was then quenched with a saturated solution of NH₄Cl (15 mL) and extracted using EtOAc (3 × 20 mL). The combined organic layers were dried over anhydrous Na₂SO₄ and concentrated affording the crude (Z)-endoxin, which was further triturated in MeOH (2 × 10 mL) to yield 11 (98%) as a white solid. ¹H NMR (400 MHz, DMSO-*d*₆) δ 9.41 (s, 1H), 7.21–7.13 (m, 2H), 7.11–7.06 (m, 3H), 7.03–6.94 (m, 2H), 6.78–6.68 (m, 4H), 6.63–6.54 (m, 2H), 3.89 (*t*, *J* = 5.5 Hz, 2H), 2.82 (*t*, *J* = 5.5 Hz, 2H), 2.41 (*q*, *J* = 7.3 Hz, 2H), 2.34 (s, 3H), 0.84 (*t*, *J* = 7.4 Hz, 3H). ¹³C NMR (101 MHz, DMSO-*d*₆) δ 156.7, 156.6, 142.7, 140.5, 138.3, 136.2, 134.4, 131.9, 130.6, 129.9, 128.4, 126.4, 115.4, 113.8, 66.3, 50.0, 35.7, 29.0, 13.9. TLC-MS (ESI) *m/z:* 374.7 [M + H]⁺; HPLC *t_{ret}* = 7.015 min.

(E)-2-(4-(1-(4-(tert-Butyldimethylsilyloxy)phenyl)-2-phenylbut-1-en-1-yl)phenoxy)-n-methylethan-1-amine (12). To compound 11 (170 mg, 0.45 mmol) dissolved in dry DCM (5 mL) excess, Et₃N (0.44 mL, 3.19 mmol, 7 equiv) was added. The mixture was cooled in an ice bath followed by the dropwise addition of *tert*-butyldimethylsilyl chloride (TBDMS-Cl) (110 mg, 0.73 mmol, 1.6 equiv) dissolved in dry DCM (1.5 mL). The reaction was left to stir until completion (approx. 3–4 h) and was then poured into a saturated aqueous solution of

NH_4Cl (15 mL) and extracted using EtOAc (4×20 mL). The organic layers were combined and dried over Na_2SO_4 , filtered, and evaporated to afford the crude material, which was purified via gradient flash chromatography using DCM/2 N NH_3 in MeOH (1–8%) to yield 205 mg (92%) of compound **12** as colorless oil. ^1H NMR (400 MHz, DMSO- d_6) δ 7.21–7.14 (m, 2H), 7.13–7.04 (m, 5H), 6.87–6.82 (m, 2H), 6.74–6.68 (m, 2H), 6.61–6.56 (m, 2H), 3.85 (t, $J = 5.6$ Hz, 2H), 2.72 (t, $J = 5.6$ Hz, 2H), 2.39 (q, $J = 7.3$ Hz, 2H), 2.28 (s, 3H), 0.96 (s, 9H), 0.84 (t, $J = 7.4$ Hz, 3H), 0.20 (s, 6H). ^{13}C NMR (101 MHz, DMSO- d_6) δ 156.5, 153.8, 142.0, 140.4, 137.5, 136.3, 135.1, 131.3, 130.2, 129.3, 127.8, 126.0, 119.4, 113.4, 66.9, 50.2, 36.1, 28.5, 25.5, 17.9, 13.3, –4.5. TLC-MS (ESI) m/z : 488.9 [M + H] $^+$; HPLC $t_{ret} = 10.389$ min.

(E)-6-(2-(2-(2-(4-(1-(4-((tert-Butyldimethylsilyl)oxy)phenyl)-2-phenylbut-1-en-1-yl)phenoxy)ethyl)(methyl)amino)ethoxy)-ethoxyethoxy)-n-(3-chloro-4-fluorophenyl)-7-methoxyquinazolin-4-amine (**13**). Compound **12** (93 mg, 0.19 mmol), compound **6b** (77 mg, 0.14 mmol, 1.1 equiv), and Et_3N (53 μL , 0.38 mmol, 3 equiv) were dissolved in dry NMP (4 mL). The reaction was heated up to 60°C and left to stir overnight. HPLC indicated almost complete consumption of reactant **12**. The reaction was quenched with saturated aqueous NH_4Cl solution (15 mL) and extracted with EtOAc (3×20 mL). The combined organic layers were washed using brine (3×15 mL), dried over Na_2SO_4 , and concentrated under reduced pressure. The crude material was subjected to column chromatography using gradient of DCM/2 N NH_3 in MeOH (1–7%) to yield 80 mg (70%) of **13** as a white foam. ^1H NMR (400 MHz, DMSO- d_6) δ 9.52 (s, 1H), 8.50 (s, 1H), 8.13 (dd, $J = 6.8$, 2.6 Hz, 1H), 7.86–7.75 (m, 2H), 7.43 (t, $J = 9.1$ Hz, 1H), 7.21 (s, 1H), 7.16–7.11 (m, 2H), 7.09–6.97 (m, 5H), 6.80 (d, $J = 8.5$ Hz, 2H), 6.65 (d, $J = 8.8$ Hz, 2H), 6.54 (d, $J = 8.8$ Hz, 2H), 4.29–4.23 (m, 2H), 3.91 (s, 3H), 3.88–3.81 (m, 4H), 3.64–3.59 (m, 2H), 3.54–3.50 (m, 2H), 3.46 (t, $J = 5.9$ Hz, 2H), 2.69–2.60 (m, 2H), 2.54–2.51 (m, 2H), 2.35 (q, $J = 7.3$ Hz, 2H), 2.20 (s, 3H), 0.94 (s, 9H), 0.81 (t, $J = 7.4$ Hz, 3H), 0.17 (s, 6H). ^{13}C NMR (101 MHz, DMSO- d_6) δ 156.4, 156.0, 154.5, 153.7, 153.1 (d, $J = 242.3$ Hz), 152.7, 148.2, 147.1, 142.0, 140.4, 137.5, 136.8 (d, $J = 3.2$ Hz), 136.3, 135.1, 131.3, 130.2, 129.3, 127.8, 126.0, 123.3, 122.1 (d, $J = 6.9$ Hz), 119.4, 118.8 (d, $J = 18.3$ Hz), 116.5 (d, $J = 21.9$ Hz), 113.4, 108.7, 107.4, 102.6, 70.0, 69.7, 68.69, 68.65, 68.3, 65.6, 56.6, 55.8, 54.9, 42.8, 28.5, 25.5, 17.9, 13.3, –4.5. TLC-MS (ESI) m/z : 945.8 [M + Na + H] $^+$; HPLC $t_{ret} = 10.905$ min.

(Z)-4-(1-(4-(2-(2-(2-(4-(3-Chloro-4-fluorophenyl)amino)-7-methoxyquinazolin-6-yl)oxy)ethoxy)ethoxyethyl)(methyl)amino)ethoxyphenyl)-2-phenylbut-1-en-1-yl)phenol (**14**). Tetrabutylammonium fluoride (1.5 equiv, ca. 1 mol/L in THF) was added dropwise into a cooled solution of **13** (77 mg, 0.08 mmol) in dry THF (4 mL). The mixture was allowed to stir at ambient temperature until conversion was complete (approx. 2 h). Extractive work-up was carried out using neutral 15 mL of phosphate-buffered saline (PBS) (0.01 M phosphate buffer, 2.7 mM KCl and 137 mM NaCl, pH 7.4 at 25°C) and diethyl ether (3×10 mL). The combined organic extracts were dried over NaSO_4 , filtered, and evaporated under reduced pressure to afford the crude product, which was directly precipitated from pentane. The white solid was collected by filtration and washed with pentane (3×) to afford compound **14** in 97% yield. ^1H NMR (400 MHz, DMSO- d_6) δ 9.53 (s, 1H), 9.40 (s, 1H), 8.51 (s, 1H), 8.13 (dd, $J = 6.8$, 2.6 Hz, 1H), 7.87–7.75 (m, 2H), 7.44 (t, $J = 9.1$ Hz, 1H), 7.21 (s, 1H), 7.18–7.02 (m, 5H), 6.93 (d, $J = 8.4$ Hz, 2H), 6.73 (d, $J = 8.5$ Hz, 2H), 6.65 (d, $J = 8.7$ Hz, 2H), 6.53 (d, $J = 8.8$ Hz, 2H), 4.30–4.22 (m, 2H), 3.92 (s, 3H), 3.85 (t, $J = 5.1$ Hz, 4H), 3.64–3.58 (m, 2H), 3.55–3.49 (m, 2H), 3.46 (t, $J = 5.9$ Hz, 2H), 2.65 (t, $J = 5.7$ Hz, 2H), 2.55–2.51 (m, 2H), 2.38 (q, $J = 7.2$ Hz, 2H), 2.20 (s, 3H), 0.82 (t, $J = 7.7$ Hz, 3H). ^{13}C NMR (101 MHz, DMSO- d_6) δ 156.2, 156.0, 156.0, 154.4, 153.1 (d, $J = 242.7$ Hz), 152.6, 148.1, 147.0, 142.2, 139.9, 137.9, 136.8 (d, $J = 2.7$ Hz), 135.4, 133.8, 131.3, 130.0, 129.3, 127.7, 125.8, 123.3, 122.1 (d, $J = 6.7$ Hz), 118.7 (d, $J = 18.4$ Hz), 116.4 (d, $J = 21.6$ Hz), 114.9, 113.2, 108.7, 107.4, 102.7, 70.0, 69.6, 68.6, 68.61, 68.3, 65.6, 56.6, 56.0, 55.8, 42.8, 28.4, 13.3. TLC-MS (ESI) m/z : 808.3 [M + H] $^+$; HRMS (ESI): calcd for $\text{C}_{46}\text{H}_{48}\text{ClFN}_4\text{O}_6$ [M + Na] $^+$ 829.32464, found 829.31453; HPLC $t_{ret} = 7.689$ min.

General Procedure for the Synthesis of Compounds **15b–d**.

To a stirred solution of the commercially available bromoalkanoic acids (1.05 equiv) and TBTU (1.5 equiv) in dry DCM (ca. 0.05 M), DIPEA (3 equiv), and amine **4** (1 equiv) suspended in dry DCM (ca. 0.1 M) were added dropwise and stirring at room temperature was continued until HPLC indicated full consumption of the reacting amine (approx. 1.5 h). The reaction was quenched with a saturated aqueous NH_4Cl solution (15 mL) and the aqueous layer extracted with DCM (3×20 mL). The combined organic layers were dried over anhydrous Na_2SO_4 and concentrated under reduced pressure. Purification of the crude material was carried out via flash chromatography to obtain the title compounds **15b–d**.

6-Bromo-N-(3-((4-(3-chloro-4-fluorophenyl)amino)-7-methoxyquinazolin-6-yl)oxy)propyl Hexanamide (15b**).** **15b** (112 mg, 67%) was obtained from 113 mg (0.29 mmol) of amine **4**, 62 mg (0.31 mmol) of 6-bromohexanoic acid, 140 mg (0.44 mmol) of TBTU, and 152 μL (0.87 mmol) of DIPEA after gradient flash chromatography purification using DCM/2 N NH_3 in MeOH (1–8%) as a yellow foam. ^1H NMR (400 MHz, DMSO- d_6) δ 9.55 (s, 1H), 8.50 (s, 1H), 8.11 (dd, $J = 6.8$, 2.6 Hz, 1H), 7.92 (t, $J = 5.4$ Hz, 1H), 7.84–7.76 (m, 2H), 7.45 (t, $J = 9.1$ Hz, 1H), 7.21 (s, 1H), 4.17 (t, $J = 6.0$ Hz, 2H), 3.95 (s, 3H), 3.49 (t, $J = 6.7$ Hz, 2H), 3.26 (dd, $J = 12.4$, 6.5 Hz, 2H), 2.08 (t, $J = 7.3$ Hz, 2H), 1.98 (dd, $J = 12.6$, 6.2 Hz, 2H), 1.82–1.72 (m, 2H), 1.51 (dt, $J = 15.0$, 7.4 Hz, 2H), 1.39–1.29 (m, 2H). ^{13}C NMR (101 MHz, DMSO- d_6) δ 172.0, 156.1, 154.6, 153.2 (d, $J = 242.7$ Hz), 152.6, 148.3, 146.8, 136.8, 123.5, 122.3 (d, $J = 6.8$ Hz), 118.8 (d, $J = 18.4$ Hz), 116.6 (d, $J = 21.6$ Hz), 108.7, 107.2, 102.6, 66.6, 55.9, 39.5, 35.6, 35.3, 35.0, 32.0, 28.8, 27.2, 24.4. TLC-MS (ESI) m/z : 553.3 [M + H] $^+$; HPLC $t_{ret} = 7.666$ min.

7-Bromo-N-(3-((4-(3-chloro-4-fluorophenyl)amino)-7-methoxyquinazolin-6-yl)oxy)propyl heptanamide (15c**).** **15c** (112 mg, 57%) was obtained from 130 mg (0.34 mmol) of amine **4**, 76 mg (0.36 mmol) of 7-bromohexanoic acid, 164 mg (0.51 mmol) of TBTU, and 178 μL (1.02 mmol) of DIPEA after gradient flash chromatography purification using DCM/2 N in NH_3 MeOH (1–8%) as a yellow foam. ^1H NMR (400 MHz, DMSO- d_6) δ 9.53 (s, 1H), 8.50 (s, 1H), 8.11 (dd, $J = 6.8$, 2.6 Hz, 1H), 7.87 (t, $J = 5.3$ Hz, 1H), 7.83–7.77 (m, 2H), 7.44 (t, $J = 9.1$ Hz, 1H), 7.21 (s, 1H), 4.17 (t, $J = 6.0$ Hz, 2H), 3.95 (s, 3H), 3.47 (t, $J = 6.7$ Hz, 2H), 3.27 (dd, $J = 12.5$, 6.5 Hz, 2H), 2.10–2.03 (m, 2H), 2.01–1.93 (m, 2H), 1.78–1.71 (m, 2H), 1.51–1.45 (m, 2H), 1.39–1.32 (m, 2H), 1.28–1.21 (m, 2H). ^{13}C NMR (101 MHz, DMSO- d_6) δ 172.2, 156.5, 155.0, 153.6 (d, $J = 243.5$ Hz), 151.9, 148.6, 136.2, 124.2, 122.9 (d, $J = 7.0$ Hz), 118.9 (d, $J = 18.4$ Hz), 116.6 (d, $J = 21.7$ Hz), 108.4, 105.7, 102.9, 66.8, 56.1, 39.5, 35.6, 35.3, 35.1, 32.1, 28.7, 27.3, 25.1. TLC-MS (ESI) m/z : 567.3 [M + H] $^+$; HPLC $t_{ret} = 8.079$ min.

10-Bromo-N-(3-((4-(3-chloro-4-fluorophenyl)amino)-7-methoxyquinazolin-6-yl)oxy)propyl Decanamide (15d**).** **15d** (91 mg, 56%) was obtained from 100 mg (0.27 mmol) of amine **4**, 70 mg (0.28 mmol) of 10-bromodecanoic acid, 130 mg (0.41 mmol) of TBTU, and 141 μL (0.81 mmol) of DIPEA after gradient flash chromatography purification using DCM/2 N NH_3 in MeOH (1–6%) as a yellow foam. ^1H NMR (400 MHz, DMSO- d_6) δ 9.55 (s, 1H), 8.50 (s, 1H), 8.12 (dd, $J = 6.8$, 2.6 Hz, 1H), 7.89 (d, $J = 5.4$ Hz, 1H), 7.84–7.77 (m, 2H), 7.44 (t, $J = 9.1$ Hz, 1H), 7.21 (s, 1H), 4.16 (t, $J = 6.0$ Hz, 2H), 3.94 (s, 3H), 3.47 (t, $J = 6.7$ Hz, 2H), 3.26 (dd, $J = 12.4$, 6.5 Hz, 2H), 2.05 (t, $J = 7.4$ Hz, 2H), 2.00–1.91 (m, 2H), 1.76–1.61 (m, 2H), 1.50–1.42 (m, 2H), 1.34–1.25 (m, 2H), 1.19 (s, 8H). ^{13}C NMR (101 MHz, DMSO- d_6) δ 172.73, 156.48, 155.00, 153.61 (d, $J = 242.8$ Hz), 153.10, 148.76, 147.45, 137.30, 123.87, 122.71 (d, $J = 6.7$ Hz), 119.25 (d, $J = 18.3$ Hz), 117.01 (d, $J = 21.5$ Hz), 109.23, 107.77, 103.05, 67.07, 56.37, 36.06, 35.93, 35.59, 32.68, 29.21, 29.19, 29.14, 29.09, 28.52, 27.93, 25.74. TLC-MS (ESI) m/z : 609.4 [M + H] $^+$; HPLC $t_{ret} = 9.718$ min.

General Procedure for the Synthesis of Compounds **16b–d**.

The silyl protected endoxifen (**12**), Et_3N (3 equiv), and compound **15b**, **15c**, or **15d** (1.05 equiv) were dissolved in dry NMP (0.04 M) under nitrogen. The reaction mixture was heated to 60°C and left to stir overnight. After almost complete consumption of the reacting amine **12** (confirmed by TLC and HPLC), the reaction was quenched with saturated aqueous NH_4Cl (15 mL) and extracted using EtOAc (3×20 mL). The combined organic layers were washed (3×15 mL)

using brine before drying over anhydrous Na_2SO_4 and evaporated under reduced pressure. Purification of the product was carried out by flash column chromatography.

(*E*)-6-(2-(4-(1-(4-(*tert*-Butyldimethylsilyl)oxy)phenyl)-2-phenylbut-1-en-1-yl)phenoxy)ethyl)(methyl)amino)-n-(3-((4-(3-chloro-4-fluorophenyl)amino)-7-methoxyquinazolin-6-yl)oxy) propyl)-hexanamide (**16b**). **16b** (72 mg, 68%) was obtained from 54 mg (0.11 mmol) of **12**, 65 mg (0.12 mmol) of **15b**, and 47 μL (0.33 mmol) of Et_3N after gradient flash chromatography purification using DCM/2 N NH_3 in MeOH (1–7%) as a yellow foam. ^1H NMR (400 MHz, $\text{DMSO}-d_6$) δ 9.55 (s, 1H), 8.50 (s, 1H), 8.12 (dd, J = 6.8, 2.5 Hz, 1H), 7.88 (t, J = 5.4 Hz, 1H), 7.83–7.78 (m, 2H), 7.43 (t, J = 9.1 Hz, 1H), 7.21 (s, 1H), 7.16 (t, J = 7.3 Hz, 2H), 7.11–7.00 (m, 5H), 6.82 (d, J = 8.4 Hz, 2H), 6.68 (d, J = 8.6 Hz, 2H), 6.55 (d, J = 8.6 Hz, 2H), 4.16 (t, J = 5.9 Hz, 2H), 3.93 (s, 3H), 3.83 (t, J = 5.8 Hz, 2H), 3.25 (dd, J = 12.3, 6.3 Hz, 2H), 2.54 (t, J = 5.9 Hz, 2H), 2.36 (q, J = 7.2 Hz, 2H), 2.25 (t, J = 7.1 Hz, 2H), 2.11 (s, 3H), 2.04 (t, J = 7.3 Hz, 2H), 1.99–1.92 (m, 2H), 1.52–1.42 (m, 2H), 1.33 (dd, J = 14.3, 7.4 Hz, 2H), 1.20 (d, J = 7.1 Hz, 2H), 0.94 (s, 9H), 0.82 (t, J = 7.4 Hz, 3H), 0.19 (s, 6H). ^{13}C NMR (101 MHz, $\text{DMSO}-d_6$) δ 172.2, 156.4, 156.0, 154.5, 153.8, 153.1 (d, J = 242.8 Hz), 152.6, 148.3, 147.0, 142.0, 140.4, 137.5, 136.9, 136.3, 135.1, 131.3, 130.2, 129.3, 127.9, 126.0, 123.4, 122.2 (d, J = 6.7 Hz), 119.4, 118.8 (d, J = 18.3 Hz), 116.5 (d, J = 21.5 Hz), 113.4, 108.8, 107.4, 102.6, 66.6, 65.6, 57.3, 55.9, 55.7, 42.3, 35.6, 35.5, 28.8, 28.5, 26.5, 25.5, 25.2, 17.9, 13.3, –4.5. TLC-MS (ESI) m/z : 961.0 [M + H]⁺; HPLC t_{ret} = 10.844 min.

(*E*)-7-(2-(4-(1-(4-(*tert*-Butyldimethylsilyl)oxy)phenyl)-2-phenylbut-1-en-1-yl)phenoxy)ethyl)(methyl)amino)-n-(3-((4-(3-chloro-4-fluorophenyl)amino)-7-methoxyquinazolin-6-yl)oxy)propyl)-heptanamide (**16c**). **16c** (72 mg, 60%) was obtained from 60 mg (0.12 mmol) of **12**, 73 mg (0.13 mmol) of **15c**, and 51 μL (0.37 mmol) of Et_3N after gradient flash chromatography purification using DCM/2 N NH_3 in MeOH (1–9%) as a yellow foam. ^1H NMR (400 MHz, $\text{DMSO}-d_6$) δ 9.54 (s, 1H), 8.50 (s, 1H), 8.12 (dd, J = 6.8, 2.6 Hz, 1H), 7.85 (t, J = 5.4 Hz, 1H), 7.83–7.77 (m, 2H), 7.43 (t, J = 9.1 Hz, 1H), 7.21 (s, 1H), 7.19–7.13 (m, 2H), 7.11–7.02 (m, 5H), 6.82 (d, J = 8.5 Hz, 2H), 6.69 (d, J = 8.8 Hz, 2H), 6.55 (d, J = 8.8 Hz, 2H), 4.16 (t, J = 6.0 Hz, 2H), 3.93 (s, 3H), 3.84 (t, J = 5.9 Hz, 2H), 3.26 (dd, J = 12.4, 6.5 Hz, 2H), 2.55 (t, J = 5.8 Hz, 2H), 2.37 (q, J = 7.3 Hz, 2H), 2.28–2.22 (m, 2H), 2.11 (s, 3H), 2.04 (t, J = 7.4 Hz, 2H), 1.97 (dd, J = 12.6, 6.3 Hz, 2H), 1.45 (dd, J = 14.1, 7.1 Hz, 2H), 1.30 (dd, J = 13.1, 6.5 Hz, 2H), 1.23–1.15 (m, 4H), 0.94 (s, 9H), 0.83 (t, J = 7.4 Hz, 3H), 0.19 (s, 3H). ^{13}C NMR (101 MHz, $\text{DMSO}-d_6$) δ 172.2, 156.4, 154.5, 153.8, 153.1 (d, J = 242.8 Hz), 152.6, 148.3, 147.0, 142.0, 140.4, 137.5, 136.8, 136.3, 135.1, 131.3, 130.2, 129.3, 127.8, 126.0, 123.4, 122.2 (d, J = 6.8 Hz), 119.4, 118.8 (d, J = 18.3 Hz), 116.5 (d, J = 21.6 Hz), 113.4, 108.8, 107.3, 102.6, 66.6, 65.6, 57.3, 55.9, 55.7, 42.3, 39.5, 35.6, 35.4, 28.7, 28.6, 28.5, 26.6, 26.5, 25.5, 25.3, 17.9, 13.3, –4.5. TLC-MS (ESI) m/z : 974.9 [M + H]⁺; HPLC t_{ret} = 10.951 min.

(*E*)-10-((2-(4-(1-(4-(*tert*-Butyldimethylsilyl)oxy)phenyl)-2-phenylbut-1-en-1-yl)phenoxy)ethyl)(methyl)amino)-n-(3-((4-(3-chloro-4-fluorophenyl)amino)-7-methoxyquinazolin-6-yl)oxy)propyl-decanamide (**16d**). **16d** (77 mg, 87%) was obtained from 54 mg (0.11 mmol) of **12**, 71 mg (0.12 mmol) of **15d**, and 47 μL (0.33 mmol) of Et_3N after gradient flash chromatography purification using DCM/2 N NH_3 in MeOH (1–7%) as a yellow foam. ^1H NMR (400 MHz, $\text{DMSO}-d_6$) δ 9.54 (s, 1H), 8.50 (s, 1H), 8.12 (dd, J = 6.8, 2.6 Hz, 1H), 7.87 (t, J = 5.4 Hz, 1H), 7.83–7.77 (m, 2H), 7.43 (t, J = 9.1 Hz, 1H), 7.24–7.13 (m, 3H), 7.12–7.02 (m, 5H), 6.82 (d, J = 8.5 Hz, 2H), 6.69 (d, J = 8.7 Hz, 2H), 6.56 (d, J = 8.8 Hz, 2H), 4.16 (t, J = 6.0 Hz, 2H), 3.93 (s, 3H), 3.85 (t, J = 5.8 Hz, 2H), 3.26 (dd, J = 12.3, 6.5 Hz, 2H), 2.55 (t, J = 5.8 Hz, 2H), 2.38 (q, J = 7.3 Hz, 2H), 2.28–2.22 (m, 2H), 2.13 (s, 3H), 2.04 (t, J = 7.4 Hz, 2H), 2.00–1.92 (m, 2H), 1.52–1.40 (m, 2H), 1.33–1.24 (m, 2H), 1.23–1.13 (m, 10H), 0.94 (s, 9H), 0.83 (t, J = 7.4 Hz, 3H), 0.19 (s, 6H). ^{13}C NMR (101 MHz, $\text{DMSO}-d_6$) δ 172.2, 156.4, 156.0, 154.5, 153.8, 153.1 (d, J = 242.7 Hz), 152.6, 148.3, 147.0, 142.0, 140.4, 137.5, 136.9, 136.3, 135.1, 131.3, 130.2, 129.3, 127.9, 126.0, 123.4, 122.2 (d, J = 6.7 Hz), 119.4, 118.8 (d, J = 18.4 Hz), 116.5 (d, J = 21.8 Hz), 113.4, 108.8, 107.3, 102.6, 66.6, 65.6, 57.4, 55.9, 55.7, 42.3, 39.5, 35.6, 35.5, 28.93, 28.92, 28.8, 28.7, 28.5, 26.8, 26.7, 25.5, 25.3,

17.9, 13.3, –4.5. TLC-MS (ESI) m/z : 1016.6 [M + H]⁺; HPLC t_{ret} = 11.509 min.

General Procedure for the Synthesis of 17b–d. To a stirred and cooled solution of the corresponding compound **16b–d** in THF (0.02 M), freshly prepared tetrabutylammonium fluoride solution (1 M in THF; 1.5 equiv) was added dropwise and left to stir at rt until TLC and HPLC indicated complete conversion. The reaction was then extracted using 15 mL of neutral PBS buffer (0.01 M phosphate buffer, 2.7 mM KCl, and 137 mM NaCl, pH 7.4 at 25 °C) and diethyl ether (3 × 15 mL). The combined organic layers were dried and concentrated under reduced pressure to afford the crude product, which was precipitated from pentane, filtered, and washed with pentane (3 × 10 mL) to obtain compounds **17b–d**.

(Z)-N-(3-((4-(3-Chloro-4-fluorophenyl)amino)-7-methoxyquinazolin-6-yl)oxy)propyl-6-((2-(4-(1-(4-hydroxyphenyl)-2-phenylbut-1-en-1-yl)phenoxy)ethyl)(methyl)amino)hexanamide (**17b**). **17b** (30 mg, 85%) was obtained from 40 mg (0.04 mmol) of **16b** and 18 μL (16 mg, 0.06 mmol) of TBAF as white solid. ^1H NMR (400 MHz, $\text{DMSO}-d_6$) δ 9.55 (s, 1H), 9.40 (s, 1H), 8.50 (s, 1H), 8.12 (dd, J = 6.7, 2.3 Hz, 1H), 7.87 (t, J = 5.2 Hz, 1H), 7.84–7.77 (m, 2H), 7.43 (t, J = 9.1 Hz, 1H), 7.21 (s, 1H), 7.15 (t, J = 7.3 Hz, 2H), 7.07 (t, J = 7.0 Hz, 3H), 6.95 (d, J = 8.3 Hz, 2H), 6.74 (d, J = 8.3 Hz, 2H), 6.68 (d, J = 8.5 Hz, 2H), 6.58–6.50 (m, 2H), 4.16 (t, J = 5.6 Hz, 2H), 3.93 (s, 3H), 3.84 (t, J = 5.6 Hz, 2H), 3.25 (dd, J = 11.9, 6.1 Hz, 2H), 2.54 (t, J = 5.7 Hz, 2H), 2.39 (dd, J = 14.4, 7.0 Hz, 2H), 2.26 (t, J = 7.0 Hz, 2H), 2.12 (s, 3H), 2.04 (t, J = 7.3 Hz, 2H), 1.99–1.92 (m, 2H), 1.47 (dt, J = 14.4, 7.2 Hz, 2H), 1.37–1.29 (m, 2H), 1.23–1.17 (m, 2H), 0.85–0.79 (m, 3H). ^{13}C NMR (101 MHz, $\text{DMSO}-d_6$) δ 172.2, 156.3, 156.1, 156.0, 154.5, 153.1 (d, J = 242.6 Hz), 152.6, 148.3, 147.0, 142.2, 139.9, 137.9, 136.8, 135.4, 133.9, 131.4, 130.1, 129.4, 127.8, 125.91, 123.4, 122.2 (d, J = 6.8 Hz), 118.8 (d, J = 18.4 Hz), 116.5 (d, J = 21.6 Hz), 114.9, 113.3, 108.8, 107.3, 102.6, 66.6, 65.6, 57.3, 55.9, 55.7, 42.3, 39.5, 35.6, 35.4, 28.7, 28.5, 26.4, 25.2, 13.4. TLC-MS (ESI) m/z : 846.7 [M + H]⁺; HRMS (ESI): calcd for $C_{49}H_{53}ClFN_5O_5$ [M + H]⁺ 846.37193, found 846.38009; HPLC t_{ret} = 8.516 min.

(Z)-N-(3-((4-(3-Chloro-4-fluorophenyl)amino)-7-methoxyquinazolin-6-yl)oxy)propyl-7-((2-(4-(1-(4-hydroxyphenyl)-2-phenylbut-1-en-1-yl)phenoxy)ethyl)(methyl)amino)heptanamide (**17c**). **17c** (52 mg, 95%) was obtained from 62 mg (0.06 mmol) of **16c** and 27 μL (25 mg, 0.09 mmol) of TBAF as a white solid. ^1H NMR (400 MHz, $\text{DMSO}-d_6$) δ 9.54 (s, 1H), 9.40 (s, 1H), 8.50 (s, 1H), 8.12 (dd, J = 6.8, 2.6 Hz, 1H), 7.86 (t, J = 5.4 Hz, 1H), 7.83–7.77 (m, 2H), 7.43 (t, J = 9.1 Hz, 1H), 7.21 (s, 1H), 7.19–7.12 (m, 2H), 7.10–7.04 (m, 3H), 6.96 (d, J = 8.4 Hz, 2H), 6.74 (d, J = 8.5 Hz, 2H), 6.68 (d, J = 8.7 Hz, 2H), 6.55 (d, J = 8.7 Hz, 2H), 4.22–4.12 (m, 2H), 3.94 (s, 3H), 3.85 (t, J = 5.8 Hz, 2H), 3.28–3.23 (m, 2H), 2.55 (t, J = 5.8 Hz, 2H), 2.39 (q, J = 7.3 Hz, 2H), 2.26 (t, J = 7.1 Hz, 2H), 2.12 (s, 3H), 2.04 (t, J = 7.4 Hz, 2H), 2.00–1.91 (m, 2H), 1.51–1.42 (m, 2H), 1.34–1.27 (m, 2H), 1.23–1.17 (m, 4H), 0.85–0.81 (m, 3H). ^{13}C NMR (101 MHz, $\text{DMSO}-d_6$) δ 172.2, 156.3, 156.1, 156.0, 154.5, 153.1 (d, J = 242.9 Hz), 152.6, 148.3, 147.0, 142.2, 139.9, 137.9, 136.8, 135.4, 133.9, 131.4, 130.1, 129.4, 127.8, 125.9, 123.4, 122.2 (d, J = 6.8 Hz), 118.8 (d, J = 18.2 Hz), 116.5 (d, J = 21.8 Hz), 114.9, 113.3, 108.8, 107.3, 102.7, 66.7, 65.6, 57.3, 55.9, 55.7, 42.3, 39.5, 35.6, 35.4, 28.7, 28.6, 28.5, 26.5, 25.3, 13.4. TLC-MS (ESI) m/z : 860.5 [M + H]⁺; HRMS (ESI): calcd for $C_{50}H_{55}ClFN_5O_5$ [M + H]⁺ 860.38758, found 860.39501; HPLC t_{ret} = 8.009 min.

(Z)-N-(3-((4-(3-Chloro-4-fluorophenyl)amino)-7-methoxyquinazolin-6-yl)oxy)propyl-10-((2-(4-(1-(4-hydroxyphenyl)-2-phenylbut-1-en-1-yl)phenoxy)ethyl)(methyl)amino)decanamide (**17d**). **17d** (65 mg, 95%) was obtained from 77 mg (0.08 mmol) of **16d** and 32 μL (30 mg, 0.11 mmol) of TBAF as a white solid. ^1H NMR (400 MHz, $\text{DMSO}-d_6$) δ 9.55 (s, 1H), 9.42 (s, 1H), 8.50 (s, 1H), 8.12 (dd, J = 6.8, 2.4 Hz, 1H), 7.93–7.77 (m, 3H), 7.43 (t, J = 9.1 Hz, 1H), 7.17 (dd, J = 18.6, 11.1 Hz, 3H), 7.07 (d, J = 7.4 Hz, 3H), 6.96 (d, J = 8.3 Hz, 2H), 6.74 (d, J = 8.4 Hz, 2H), 6.69 (d, J = 8.6 Hz, 2H), 6.55 (d, J = 8.6 Hz, 2H), 4.16 (t, J = 5.7 Hz, 2H), 3.94 (s, 3H), 3.86 (t, J = 5.7 Hz, 2H), 3.26 (dd, J = 12.1, 6.2 Hz, 2H), 2.56 (t, J = 5.6 Hz, 2H), 2.40 (dd, J = 14.5, 7.1 Hz, 2H), 2.25 (t, J = 7.1 Hz, 2H), 2.13 (s, 3H), 2.05 (t, J = 7.3 Hz, 2H), 1.99–1.92 (m, 2H), 1.50–1.41 (m, 2H), 1.32–1.26 (m, 2H), 1.22–1.12 (m, 10H), 0.85–0.81 (m, 3H). ^{13}C NMR (101 MHz, $\text{DMSO}-d_6$) δ

172.2, 156.3, 156.1, 156.0, 154.5, 153.1 (d, $J = 242.7$ Hz), 152.6, 148.3, 147.0, 142.2, 139.9, 137.9, 136.9, 135.4, 133.9, 131.4, 130.1, 129.4, 127.9, 125.9, 123.4, 122.2 (d, $J = 6.8$ Hz), 118.8 (d, $J = 18.3$ Hz), 116.5 (d, $J = 21.6$ Hz), 114.9, 113.3, 108.8, 107.3, 102.6, 66.6, 65.6, 57.4, 55.9, 55.7, 42.3, 39.5, 35.6, 35.5, 28.94, 28.93, 28.8, 28.73, 28.66, 28.5, 26.8, 26.7, 25.3, 13.4. TLC-MS (ESI) m/z : 902.4 [M + H]⁺; HRMS (ESI): calcd for C₅₃H₆₁ClFN₅O₅ [M + H]⁺ 902.43453, found 902.44196; HPLC t_{ret} = 8.507 min.

ER α -Radioligand Binding Assay. *In vitro* ER α binding affinity assay was conducted by Eurofins Cerep, France, as previously reported.²⁵ Briefly, ER α pre-transfected SF9 cells were incubated with 0.5 nM [³H]-estradiol for 120 min at RT in the absence and presence of hybrid ligands at four different concentrations with 10-fold dilution steps in duplicates starting with 1 μ M. Results were expressed as % binding inhibition. Results showing an inhibition (or stimulation for assays run in basal conditions) higher than 50% are considered to represent significant effects of the test compounds.

ER α Luciferase Reporter Assay. Activation assays for human ER α (NR3A1, FL) were performed in C3A cells cultured on 96-well plates in DMEM (Gibco 11,880, Invitrogen), containing 5% charcoal stripped FBS (Biowest S181F), 2 mM L-glutamine (Biowest X0550) and 1% antibiotics (Biowest L0022) at density of 6.25×10^4 cells/cm². The cells were transfected with 20 ng pCMV β , 5 ng pSG5-hER α , and 75 ng pGL3-ERE2-TATA-luciferase using calcium phosphate precipitation essentially as described before.^{26,27} After transfection of 4 h, the medium was replaced with fresh DMEM complemented with 5% charcoal stripped FBS (Biowest S181F) and including DMSO (Sigma D8418, 0.1% v/v) or EtOH (0.1% v/v), positive control 17 β -estradiol (E2, Sigma E2758), and the test compounds.

After 24 h of exposure, the cells were disrupted in lysis buffer (25 mM glycylglycine, 15 mM MgSO₄, 4 mM EGTA, 1% Triton X-100, pH 7.8, supplemented with dithiothreitol and phenylmethyl sulfonyl fluoride) and analyzed for luciferase and β -galactosidase activities using a Victor2 multiplate reader.²⁶ The raw luciferase activities were normalized to β -galactosidase activities to control for differences in transfection efficiency and cell loss to generate relative luminescence units. Hybrid compounds did not activate the single transfected C3A cell-line with only the luciferase plasmid.

Relative luminescence units were normalized against the DMSO treated samples and compared with the E2 (10 nM) treated positive control, expressed as activity %. Data are presented as mean \pm SEM (at least $n = 2$), generated from three experimental replicates. Normalized values were fitted to a non-linear model (four parameters) and relative IC₅₀ values were calculated using GraphPad Prism v9.3.

EGFR-Inhibition Assay. Inhibition data (IC₅₀) against EGFR-wild type were obtained at Reaction Biology Corp. (Malvern, PA, USA) via the commercial radiolabeled ³³P(ATP) kinase activity assay. IC₅₀ values were measured in duplicates at five different concentrations with 10-fold dilution steps starting from 10 or 1 μ M. Staurosporine was tested as control compound at 10 different concentrations with a 4-fold dilution starting at 20 μ M. Reactions were carried out at 1 μ M ATP. A detailed description of the assay is given in the literature.^{31,32}

Cell Culture. MCF-7, MDA-MB-231, MDA-MB-468, and BT-549 cells were obtained from American Type Culture Collection (ATCC, Manassas, VA) or DSMZ. Cells were cultured in DMEM:F12 containing 10% fetal bovine serum (FBS) and 1% penicillin/streptomycin +1% sodium pyruvate at 37 °C in a humidified atmosphere with 5% CO₂. Cells were passaged when they reached 80% confluence. TamR MCF-7 cells were cultured in the same condition (10% FBS and 1% penicillin/streptomycin at 37 °C in a humidified atmosphere with 5% CO₂) using RPMI-1640 medium. The development and characterization of TamR MCF-7 cells are described.¹⁴

Cell Viability Assay. The MTT assay method was used to determine cellular viability following exposure to each of the drug conjugates 5a–e, 7a,b, 14, and 17b–d or controls tamoxifen, 4-OH-tamoxifen, endoxifen, and gefitinib (alone or in combination) as described.¹⁴ Sub-confluent monolayer cell lines, MCF-7, TamR MCF-7, MDA-MB-231, MDA-MB-468, and BT-549, grown on 10 cm culture plates, were trypsinized, plated equally into each well of a 96-well plate. The next day, cells were exposed to each of the drugs or drug conjugates

(1 nM, 10 nM, 100 nM, 1 μ M, 10 μ M, or 100 μ M) for 24 h. Next, 10 μ L MTT (5 or 0.5 mg/mL final concentration) (Sigma-Aldrich, St. Louis, MO) was added to each well and the plates were placed in the incubator for 4 h (5% CO₂ and 37 °C). Following the treatment period, the medium was aspirated, and 100 μ L DMSO (Fisher Scientific, Pittsburgh, PA) was added to each well to stop the reaction. The plate was wrapped in aluminum foil and incubated at room temperature for 15 min to dissolve the MTT-formazan crystals. The absorbance was measured at 570 nm (Synergy HTX Multi-Mode Microplate Reader, BioTek). Additionally, for compounds 5b, 5c, 17b, and 17c, an XTT (catalog: X6493) assay was applied to analyze cell viability after 5 days treatment per the manufacturer's protocol. In both cases, potency (IC₅₀ or EC₅₀) values were calculated from individual curves generated by nonlinear regression analysis (four parameters) least sum of squares (GraphPad Software, La Jolla, CA).

Crystal Violet Staining. A total of 5000 cells/well were split into 24-well plates and treated with indicated compounds under different concentrations for 5 days. Cells were washed once with PBS, fixed with 4% paraformaldehyde, and then stained with crystal violet solution (Sigma, HT901).

Western Blot. *WB Determining the Basal Expression Levels of EGFR and ER α upon Short Treatment Time.* Cell were washed with PBS twice and then lysed in RIPA lysis buffer (50 mM Tris pH 8.0, 150 mM, NaCl, 1% NP-40, 0.5% Sodium deoxycholate, 0.1% sodium dodecyl sulfate) supplemented with phosphatase and protease inhibitors (cComplete and PhosSTOP tablets, Roche). Protein concentration was determined using the DC-protein Assay Kit (Bio-Rad, Catalog: 5000111). Proteins were resolved by sodium dodecyl sulfate-polyacrylamide gel electrophoresis (SDS-PAGE) and transferred to polyvinylidene difluoride (PVDF) membranes (Millipore). Membranes were immunoblotted with antibodies against Vinculin (Sigma, V9193), Estrogen Receptor α (Cell Signaling Technology, #8644), and EGF Receptor (Cell Signaling Technology, #4267). Blots were washed with TBST and incubated with horseradish peroxidase AffiniPure Goat Anti-Mouse IgG + IgM (H + L) (Jackson ImmunoResearch, 115-035-068) or horseradish AffiniPure Goat Anti-Rabbit IgG (H + L) (Jackson ImmunoResearch, 111-035-045), developed with Clarity and Clarity Max ECL Western Blotting Substrates (Bio-rad, 1705060) and imaged with ChemiDoc MP system (Biorad).

WB Determining the Basal Expression Levels of EGFR. To determine if breast cancer cell lines, MMC (HER2/neu), MCF-7 (ER+), MDA-MB-231 (TNBC), and BT-549 (TNBC) expressed EGFR, western blotting was performed using the Odyssey Western Blotting Kit IV RD (LI-COR Biosciences, USA) as described¹⁴ with modification. Briefly, cells, grown to ~80% confluence, were washed with 1× sterile PBS, scraped into 100 μ L cell lysis buffer (1× Laemmli sample buffer +5% β -mercaptoethanol; BioRad, USA) containing protease inhibitors (Complete Mini Protease Inhibitor Cocktail; Roche), transferred to a microtube, and stored at -20 °C until use. Samples (20 μ L) or molecular weight markers (1 μ L; Precision Plus Protein, BioRad, USA) were loaded into wells and then subjected to SDS-PAGE (8% SDS-polyacrylamide gel). Proteins were transferred to nitrocellulose membranes (Odyssey Nitrocellulose Membrane; LI-COR Biosciences, USA) and incubated with Revert 700 Total Protein Stain (LI-COR Bioscience, USA) for 4 min followed by washing twice using Revert Wash Solution (LI-COR Bioscience, USA) for 45 s at 25 °C to remove residual stain. Total protein levels were visualized and quantified per manufacturer's instructions using the Odyssey Infrared Imager and software (LI-COR Biosciences, USA). Following total protein analyses, membranes were washed once with 5 mL 1× PBS for 5 min and then placed in Odyssey Blocking Buffer (LI-COR Biosciences, USA) containing 0.1% Tween 20 for 1 h with gentle rocking at 25 °C. The blocking solution was removed, and membranes were then incubated overnight at 4 °C with anti-EGFR (A-10) primary antibody (1:1000; sc-373746, Santa Cruz Biotechnology, Dallas, TX) in 10 mL blocking buffer containing 0.1% Tween 20 with gentle rocking. The next day, blots were washed thrice (5 min per wash) at 25 °C with PBS-Tween 20 (0.1%) solution followed by incubation for 45 min at 25 °C with 10 mL blocking buffer containing 0.1% Tween 20 and secondary antibody (1:20,000; goat anti-mouse IRDye 800CW; LI-COR Bioscience, USA).

Following incubation with secondary antibody, the solution was decanted, and the membranes were washed four times with the first three washes in 1× PBS and 0.1% Tween 20 and the final wash in 1× PBS. Bands were quantified using the Odyssey Infrared Imaging System (LI-COR Bioscience, USA) and then normalized by total protein. Full blots of protein bands and total proteins can be found in the SI (Figure S6).

Metabolic Stability Studies. Pooled male mice liver microsomes were purchased from Xenotech. Incubation of test compounds (100 μM) was done in the presence of an NADPH-regenerating system (5 mM glucose-6-phosphate, 5 U/mL glucose-6-phosphate dehydrogenase, and 1 mM NADP $^+$) and 4 mM MgCl₂·6 H₂O in 0.1 M Tris buffer (pH 7.4) for 5 min at 37 °C and 750 rpm on a shaker. The incubation mixture was split into 50 μL aliquots, and the reaction time was calculated starting from the addition of the mouse liver microsomes. The reaction was quenched at several time intervals (0, 10, 20, 30, 60, 90, and 120 min) using 100 μL (50 μM in MeCN) of an internal standard. After vortexing and centrifuging the samples, the supernatant was directly used for LC-MS quantitative analysis. The incubation step was conducted in triplicates for every compound and a maximum of 1% organic solvent was not surpassed. An Alliance 2695 HPLC (Waters GmbH, Eschborn) equipped with a Phenomenex Kinetex column with the following specifications (2.6 μm , C18, 100 Å, 100 × 3.00 mm) was used for sample separation with the gradient set to: 0–2.5 min 10% B, 2.5–12.5 min from 10 to 50% B, 12.5–15 min 50% B, and 15.01–18 min from 50 to 10% B at a flow rate of 0.6 mL/min. Mobile phase A: 90% H₂O water, 10% acetonitrile, and additional 0.1% formic acid (v/v); mobile phase B: acetonitrile with 0.1% formic acid (v/v). Samples' temperature were maintained at 10 °C, and the column temperature was set to 40 °C with 5 μL injection volume. The Micromass Quattro micro triple quadrupole mass spectrometer (Waters GmbH, Eschborn) was used for detection using electrospray ionization (+ve mode). Voltages for the spray, cone, extractor, and RF lens were adjusted to 4 kV, 30 V, 5 V, and 1 V, respectively. The desolvation temperature and gas flow were set to 350 °C and 650 L/h respectively. MassLynx 4.1 was used for data analysis.

ASSOCIATED CONTENT

Supporting Information

The Supporting Information is available free of charge at <https://pubs.acs.org/doi/10.1021/acs.jmedchem.1c01646>.

Experimental procedures for the synthesis of compounds 8 and 9, ¹H NMR and ¹³C NMR spectra for all drug conjugates, HPLC traces for all drug conjugates, dose-response curves for the ER α luciferase reporter assay, dose-response curves for the EGFR inhibition assay, concentration-response curves for the cell viability assays, Western Blot to determine ER α and EGFR levels upon compound treatment, Western Blot to determine the basal expression of EGFR, and predicted ADME properties for selected compounds ([PDF](#))

Molecular formula strings ([CSV](#))

AUTHOR INFORMATION

Corresponding Authors

Darius P. Zlotos – Department of Pharmaceutical Chemistry, Faculty of Pharmacy and Biotechnology, The German University in Cairo, 11835 New Cairo City, Cairo, Egypt; [orcid.org/0000-0002-1193-3119](#); Email: darius.zlotos@guc.edu.eg

Stefan A. Laufer – Department of Pharmaceutical/Medicinal Chemistry, Eberhard Karls University Tübingen, 72076 Tübingen, Germany; Cluster of Excellence iFIT (EXC 2180) 'Image-Guided & Functionally Instructed Tumor Therapies', University of Tübingen, 72076 Tübingen, Germany; Center for Academic Drug Discovery, 72076 Tübingen,

Germany; [orcid.org/0000-0001-6952-1486](#); Email: stefan.laufer@uni-tuebingen.de

Authors

Carine M. Abdelmalek – Department of Pharmaceutical Chemistry, Faculty of Pharmacy and Biotechnology, The German University in Cairo, 11835 New Cairo City, Cairo, Egypt; Department of Pharmaceutical/Medicinal Chemistry, Eberhard Karls University Tübingen, 72076 Tübingen, Germany

Zexi Hu – Department of Medical Oncology and Pneumology (Internal Medicine VIII), University Hospital of Tübingen, 72076 Tübingen, Germany; Cluster of Excellence iFIT (EXC 2180) 'Image-Guided & Functionally Instructed Tumor Therapies', University of Tübingen, 72076 Tübingen, Germany

Thales Kronenberger – Department of Pharmaceutical/Medicinal Chemistry, Eberhard Karls University Tübingen, 72076 Tübingen, Germany; Department of Medical Oncology and Pneumology (Internal Medicine VIII), University Hospital of Tübingen, 72076 Tübingen, Germany; Cluster of Excellence iFIT (EXC 2180) 'Image-Guided & Functionally Instructed Tumor Therapies', University of Tübingen, 72076 Tübingen, Germany; [orcid.org/0000-0001-6933-7590](#)

Jenni Küblbeck – A.I. Virtanen Institute for Molecular Sciences, University of Eastern Finland, FI-70210 Kuopio, Finland; School of Pharmacy, University of Eastern Finland, FI-70210 Kuopio, Finland

Franziska J. M. Kinnen – Department of Pharmaceutical/Medicinal Chemistry, Eberhard Karls University Tübingen, 72076 Tübingen, Germany

Salma S. Hesse – Department of Pharmaceutical Chemistry, Faculty of Pharmacy and Biotechnology, The German University in Cairo, 11835 New Cairo City, Cairo, Egypt

Afsin Malik – School of Pharmacy, Division of Pharmaceutical, Administrative and Social Sciences, Duquesne University, Pittsburgh, Pennsylvania 15282, United States

Mark Kudolo – Department of Pharmaceutical/Medicinal Chemistry, Eberhard Karls University Tübingen, 72076 Tübingen, Germany

Raimund Niess – Department of Pharmaceutical/Medicinal Chemistry, Eberhard Karls University Tübingen, 72076 Tübingen, Germany

Matthias Gehringer – Department of Pharmaceutical/Medicinal Chemistry, Eberhard Karls University Tübingen, 72076 Tübingen, Germany; Cluster of Excellence iFIT (EXC 2180) 'Image-Guided & Functionally Instructed Tumor Therapies', University of Tübingen, 72076 Tübingen, Germany; [orcid.org/0000-0003-0163-3419](#)

Lars Zender – Department of Medical Oncology and Pneumology (Internal Medicine VIII), University Hospital of Tübingen, 72076 Tübingen, Germany; Cluster of Excellence iFIT (EXC 2180) 'Image-Guided & Functionally Instructed Tumor Therapies', University of Tübingen, 72076 Tübingen, Germany

Paula A. Witt-Enderby – School of Pharmacy, Division of Pharmaceutical, Administrative and Social Sciences, Duquesne University, Pittsburgh, Pennsylvania 15282, United States; [orcid.org/0000-0002-1844-4457](#)

Complete contact information is available at:

<https://pubs.acs.org/doi/10.1021/acs.jmedchem.1c01646>

Notes

The authors declare no competing financial interest.

ACKNOWLEDGMENTS

This work was partially funded by Bundesministerium für Bildung und Forschung (BMBF), Deutscher Akademischer Austauschdienst (DAAD) and by the German Research Foundation (Deutsche Forschungsgemeinschaft, DFG) under Germany's Excellence Strategy-EXC 2180—390900677.

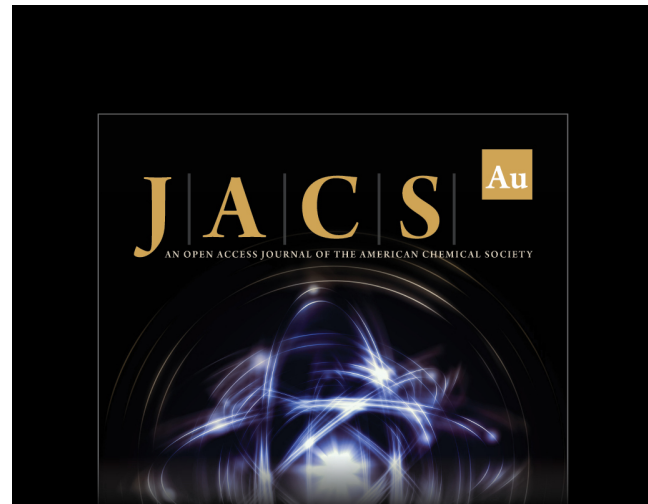
ABBREVIATIONS USED

ADC, antibody-drug conjugates; DCM, dichloromethane; DIAD, diisopropyl azodicarboxylate; DIPEA, diisopropylethylamine; DMF, dimethylformamide; EGFR, epidermal growth factor receptor; ER, estrogen receptor; ER α , estrogen receptor alpha; ERE, estrogen responsive element; ER+, estrogen-receptor positive; HDAC, histone deacetylase inhibitor; HER1, human epidermal growth factor receptor 1; HER2, human epidermal growth factor receptor 2; HERG, human ether-a-go-go related gene; IGFR, insulin-like growth factor receptor; MTT, [3-(4,5-dimethylthiazol-2-yl)-2,5-diphenyltetrazolium bromide; NMP, N-methylpyrrolidone; PDB, Protein Data Bank; PR, progesterone; TBAB, tetrabutylammonium bromide; TBAF, tetrabutylammonium fluoride; TBTU, 2-(1H-benzotriazole-1-yl)-1,1,3,3-tetramethylaminium tetrafluoroborate; TFA, trifluoric acid; TMS, trimethylsilyl; TNBC, triple-negative breast cancer

REFERENCES

- (1) Fortin, S.; Bérubé, G. Advances in the development of hybrid anticancer drugs. *Expert Opin. Drug Discovery* **2013**, *8*, 1029–1047.
- (2) Kerru, N.; Singh, P.; Koorbanally, N.; Raj, R.; Kumur, V. Recent advances (2015–2016) in anticancer hybrids. *Eur. J. Med. Chem.* **2017**, *142*, 179–212.
- (3) Ivasiv, V.; Albertini, C.; Gonzalves, A. E.; Rossi, M.; Bolognesi, M. L. Molecular hybridization as a tool for designing multitarget drug candidates for complex diseases. *Curr. Top. Med. Chem.* **2019**, *19*, 1694–1711.
- (4) Kucuksayan, E.; Ozben, T. Hybrid compounds as multitarget directed anticancer agents. *Curr. Top. Med. Chem.* **2017**, *17*, 907–918.
- (5) Tsuchikama, K.; An, Z. Antibody-drug conjugates: recent advances in conjugation and linker chemistries. *Protein Cell.* **2018**, *9*, 33–46.
- (6) *Anticancer Hybrids*; National Library of Medicine <https://pubmed.ncbi.nlm.nih.gov/?term=anticancer+hybrids>
- (7) Cai, X.; Zhai, H.; Wang, J.; Forrester, J.; Qu, H.; Yin, L.; Lai, C.; Bao, R.; Qian, C. Discovery of 7-(4-(3-ethynylphenylamino)-7-methoxyquinazolin-6-yloxy)-N-hydroxyheptanamide (CUDC-101) as a potent multi-acting HDAC, EGFR, and HER2 inhibitor for the treatment of cancer. *J. Med. Chem.* **2010**, *53*, 2000–2009.
- (8) *CUDC 101*; Springer, <https://adisinsight.springer.com/drugs/800028795>.
- (9) Hasan, M.; Leak, R. K.; Stratford, R.; Zlotos, D. P.; Witt-Enderby, P. A. Drug conjugates—an emerging approach to treat breast cancer. *Pharmacol Res Perspect.* **2018**, No. e00417.
- (10) Anderson, W. F.; Chatterjee, N.; Ershler, W. B.; Brawley, O. W. Estrogen receptor breast cancer phenotypes in the surveillance, epidemiology, and end results database. *Breast Cancer Res. Treat.* **2002**, *76*, 27–36.
- (11) Jones, M. E.; van Leeuwen, F. E.; Hoogendoorn, W. E.; Mourits, M. J. E.; Hollema, H.; van Boven, H.; Swerdlow, A. J. Endometrial cancer survival after breast cancer in relation to tamoxifen treatment: Pooled results from three countries. *Breast Cancer Res.* **2012**, *14*, R91.
- (12) Ring, A.; Dowsett, M. Mechanisms of tamoxifen resistance. *Endocr.-Relat. Cancer* **2004**, *11*, 643–658.
- (13) Burke, P. J.; Koch, T. H. Design, synthesis, and biological evaluation of doxorubicin-formaldehyde conjugates targeted to breast cancer cells. *J. Med. Chem.* **2004**, *47*, 1193–1206.
- (14) Hasan, M.; Marzouk, M. A.; Adhikari, S.; Wright, T. D.; Miller, B. P.; Matossian, M. D.; Elliot, S.; Wright, M.; Alzoubi, M.; Collins-Burow, B. M.; Burow, M.; Holzgrabe, U.; Zlotos, D. P.; Stratford, R. E.; Witt-Enderby, P. A. Pharmacological, mechanistic and pharmacokinetic assessment of novel melatonin-tamoxifen drug conjugates as breast cancer drugs. *Mol. Pharmacol.* **2019**, *96*, 272–296.
- (15) Gryder, B. E.; Rood, M. K.; Johnson, K. A.; Vishal, P.; Raftery, E. D.; Yao, L.-P. D.; Rice, M.; Azizi, B.; Doyle, D. F.; Oyelere, A. K. Histone deacetylase inhibitors equipped with estrogen receptor modulation activity. *J. Med. Chem.* **2013**, *56*, 5782–5796.
- (16) Palermo, A. F.; Diennet, M.; El Ezzyb, M.; Williams, B. M.; Cotnoir-White, D.; Mader, S.; Gleason, J. L. Incorporation of histone deacetylase inhibitory activity into the core of tamoxifen—a new hybrid design paradigm. *Bioorg. Med. Chem.* **2018**, *26*, 4428–4440.
- (17) García-Aranda, M.; Redondo, M. Protein kinase targets in breast cancer. *Int. J. Mol. Sci.* **2017**, *18*, 2543.
- (18) Knowlden, J. M.; Hutcheson, I. R.; Barrow, D.; Gee, J. M.; Nicholson, R. I. Insulin-like growth factor-i receptor signaling in tamoxifen-resistant breast cancer: A supporting role to the epidermal growth factor receptor. *Endocrinology* **2005**, *146*, 4609–4618.
- (19) Jin, K.; Kong, X.; Shah, T.; Penet, M. F.; Wildes, F.; Sgroi, D. C.; Ma, X. J.; Huang, Y.; Kallioniemi, A.; Landberg, G.; Bieche, I.; Wu, X.; Lobie, P. E.; Davidson, N. E.; Bhujwalla, Z. M.; Zhu, T.; Sukumar, S. The hoxb7 protein renders breast cancer cells resistant to tamoxifen through activation of the egfr pathway. *Proc. Natl. Acad. Sci. U. S. A.* **2012**, *109*, 2736–2741.
- (20) Massarweh, S.; Osborne, C. K.; Creighton, C. J.; Qin, L.; Tsimelzon, A.; Huang, S.; Weiss, H.; Rimawi, M.; Schiff, R. Tamoxifen resistance in breast tumors is driven by growth factor receptor signalling with repression of classic estrogen receptor genomic function. *Cancer Res.* **2008**, *68*, 826–833.
- (21) Zhang, X.; Zhang, B.; Liu, J.; Li, C.; Dong, W.; Fang, S.; Li, M.; Song, B.; Tang, B.; Wang, Z.; Zhang, Y. Mechanism of gefitinib-mediated reversal of tamoxifen resistance in MCF-7 breast cancer cells by inducing ER α re-expression. *Sci. Rep.* **2015**, *5*, 7835.
- (22) Jeong, Y.; Bae, S. Y.; You, D.; Jung, S. P.; Choi, H. J.; Kim, I.; Lee, S. K.; Yu, J.; Kim, S. W.; Lee, J. E.; Kim, S.; Nam, S. J. EGFR is a therapeutic target in hormone receptor-positive breast cancer. *Cell. Physiol. Biochem.* **2019**, *53*, 805–819.
- (23) Hesham, H. M.; Lasheen, D. S.; Abouzid, K. A. M. Comprehensive review for anticancer hybridized multitargeting HDAC inhibitors. *Med. Res. Rev.* **2018**, *1*–52.
- (24) Alam, M.; Hassan, H. E.; Kwan, Y. H.; Lee, H. J.; Kim, N. Y.; Min, K. H.; Lee, S.-Y.; Kim, D.-H.; Lee, Y. S. Design, synthesis and evaluation of alkylphosphocholin-gefitinib conjugates as multitarget anticancer agents. *Arch. Pharmacal Res.* **2018**, *41*, 35–45.
- (25) Obourn, J. D.; Koszewski, N. J.; Notides, A. C. Hormone- and DNA-binding mechanisms of the recombinant human estrogen receptor. *Biochemistry* **1993**, *32*, 6229–6236.
- (26) Pulkkinen, J. T.; Honkakoski, P.; Peräkylä, M.; Berczi, I.; Laatikainen, R. Synthesis and evaluation of estrogen agonism of diaryl 4,5-dihydroisoazoles, 3-hydroxyketones, 3-methoxyketones, and 1,3-diketones: a compound set forming a 4D molecular library. *J. Med. Chem.* **2008**, *51*, 3562–3571.
- (27) Küblbeck, J.; Jyrkkälinne, J.; Molnár, F.; Kunigas, T.; Patel, J.; Windshügel, B.; Nevalainen, T.; Laitinen, T.; Sippl, W.; Poso, A.; Honkakoski, P. New in vitro tools to study human constitutive androstane receptor (CAR) biology: discovery and comparison of human CAR inverse agonists. *Mol. Pharmaceutics* **2011**, *8*, 2424–2433.
- (28) Sanchez-Spitman, A. B.; Swen, J. J.; Dezentje, V. O.; Moes, D. J. A. R.; Gelderblom, H.; Guchelaar, H. J. Clinical pharmacokinetics and pharmacogenetics of tamoxifen and endoxifen. *Expert Rev. Clin. Pharmacol.* **2019**, *12*, 523–536.
- (29) Lien, E. A.; Solheim, E.; Lea, O. A.; Lundgren, S.; Kvinnslund, S.; Ueland, P. M. Distribution of 4-hydroxy-N-desmethyltamoxifen and

- other tamoxifen metabolites in human biological fluids during tamoxifen treatment. *Cancer Res.* **1989**, *49*, 2175–2183.
- (30) Milroy, L. G.; Koning, B.; Scheppingen, D. S. V.; Jager, N. G. L.; Beijnen, J. H.; Koek, J.; Brunsvelde, L. A multi-gram-scale stereoselective synthesis of Z-endoxifen. *Bioorg. Med. Chem. Lett.* **2018**, *28*, 1352–1356.
- (31) Duong-Ly, K. C.; Peterson, J. R. A High-throughput radiometric kinase assay. *Methods Mol. Biol.* **2016**, *1360*, 87–95.
- (32) Anastassiadis, T.; Deacon, S. W.; Devarajan, K.; Ma, H.; Peterson, J. R. Comprehensive assay of kinase catalytic activity reveals features of kinase inhibitor selectivity. *Nat. Biotechnol.* **2011**, *29*, 1039–1045.
- (33) Wakeling, A. E.; Guy, S. P.; Woodburn, J. R.; Ashton, S. E.; Curry, B. J.; Barker, A. J.; Gibson, K. H. ZD1839 (Iressa): an orally active inhibitor of epidermal growth factor signaling with potential for Cancer Therapy. *Cancer Res.* **2002**, *62*, 5749–5754.
- (34) Li, Y.; Song, Z.; Jin, Y.; Tang, Z.; Kang, J.; Ma, X. Novel selective and potent EGFR inhibitor that overcomes T790M-mediated resistance in non-small cell lung cancer. *Molecules* **2016**, *21*, 1462.
- (35) Kitagawa, D.; Yokota, K.; Gouda, M.; Narumi, Y.; Ohmoto, H.; Nishiwaki, E.; Akita, K.; Kirii, Y. Activity-based kinase profiling of approved tyrosine kinase inhibitors. *Genes Cells* **2013**, *18*, 110–122.
- (36) Günther, M.; Lategahn, J.; Juchum, M.; Döring, E.; Keul, M.; Engel, J.; Tumbrink, H. L.; Rauh, D.; Laufer, S. Trisubstituted pyridinylimidazoles as potent inhibitors of the clinically resistant L858R/T790M/C797S EGFR mutant: targeting of both hydrophobic regions and the phosphate binding site. *J. Med. Chem.* **2017**, *60*, 5613–5637.
- (37) Allred, D. C.; Brown, P.; Medina, D. The origins of estrogen receptor alpha-positive and estrogen receptor alpha-negative human breast cancer. *Breast Cancer Res.* **2004**, *6*, 240–245.
- (38) Howell, A. The future of fulvestrant ("Faslodex"). *Cancer Treat. Rev.* **2005**, *31*, S26–S33.
- (39) Wijayaratne, A. L.; Nagel, S. C.; Paige, L. A.; Christensen, D. J.; Norris, J. D.; Fowlkes, D. M.; McDonnell, D. P. Comparative analyses of mechanistic differences among antiestrogens. *Endocrinology* **1999**, *140*, 5828–5840.
- (40) Wang, L.; Guillen, V. S.; Sharma, N.; Flessa, K.; Min, J.; Carlson, K. E.; Toy, W.; Braqi, S.; Katzenellenbogen, B. S.; Katzenellenbogen, J. A.; Chandrarapthy, S.; Sharma, A. New class of selective estrogen receptor degraders (SERDs): expanding the toolbox of PROTAC Degrons. *ACS Med. Chem. Lett.* **2018**, *9*, 803–808.
- (41) Shoda, T.; Okuhira, K.; Kato, M.; Demizu, Y.; Inoue, H.; Naito, M.; Kurihara, M. Design and synthesis of tamoxifen derivatives as a selective estrogen receptor down-regulator. *Bioorg. Med. Chem. Lett.* **2014**, *24*, 87–89.
- (42) Shoda, T.; Kato, M.; Harada, R.; Fujisato, T.; Okuhira, K.; Demizu, Y.; Inoue, H.; Naito, M.; Kurihara, M. Synthesis and evaluation of tamoxifen derivatives with a long alkyl side chain as selective estrogen receptor down-regulators. *Bioorg. Med. Chem.* **2015**, *23*, 3091–3096.
- (43) Chavez, K. J.; Garimella, S. V.; Lipkowitz, S. Triple negative breast cancer cell lines: one tool in the search for better treatment of triple negative breast cancer. *Breast Dis.* **2011**, *32*, 35–48.
- (44) Foulkes, W. D.; Smith, I. E.; Reis-Filho, J. S. Triple-negative breast cancer. *N. Engl. J. Med.* **2010**, *363*, 1938–1948.
- (45) Changavi, A. A.; Shashikala, A.; Ramji, A. S. Epidermal growth factor receptor expression in triple negative and nontriple negative breast carcinomas. *J. Lab. Physicians* **2015**, *7*, 79–83.
- (46) Daurio, N. A.; Tuttle, S. W.; Worth, A. J.; Song, E. Y.; Davis, J. M.; Snyder, N. W.; Blair, I. A.; Koumenis, C. AMPK activation and metabolic reprogramming by tamoxifen through estrogen receptor-independent mechanisms suggests new uses for this therapeutic modality in cancer treatment. *Cancer Res.* **2016**, *76*, 3295–3306.
- (47) Bolanz, K. A.; Kovacs, G. G.; Landowski, C. P.; Hediger, M. A. Tamoxifen inhibits TRPV6 activity via estrogen receptor-independent pathways in TRPV6-expressing MCF-7 breast cancer cells. *Mol. Cancer Res.* **2009**, 2000–2010.
- (48) Olofson, R. A.; Martz, J. T.; Senet, J. P.; Piteau, M.; Malfroot, T. A new reagent for the selective, high-yield *N*-dealkylation of tertiary amines: improved syntheses of naltrexone and nalbuphine. *J. Org. Chem.* **1984**, *49*, 2081–2082.



J | A | C | S
AN OPEN ACCESS JOURNAL OF THE AMERICAN CHEMICAL SOCIETY

Editor-in-Chief
Prof. Christopher W. Jones
Georgia Institute of Technology, USA

Open for Submissions 

pubs.acs.org/jacsau ACS Publications
Most Trusted. Most Cited. Most Read.